Propagation of Electromagnetic Waves in Plasmas

DONALD F. DUBOIS,* VICTOR GILINSKY, AND MARGARET G. KIVELSON
The RAND Corporation, Santa Monica, California

(Received 31 August 1962; revised manuscript received 17 December 1962)

Green's function techniques are used to treat the propagation of electromagnetic waves in uniform, weakly interacting plasmas near equilibrium in the absence of external magnetic fields. The frequency and the damping of electromagnetic waves in a medium are related to the local complex conductivity tensor, which is calculated by the diagrammatic techniques of modern field theory. Physical quantities are calculated in terms of a consistent many-particle perturbation expansion in powers of a (weak) coupling parameter. An open-diagram technique is introduced which simplifies the calculation of absorptive parts. For long-wavelength longitudinal waves (i.e., electron plasma oscillations) it is found that the main absorption mechanism in the electron-ion plasma is the two-particle collision process appropriately corrected for collective effects and not the one-particle (or Landau) damping process. Electron-ion collisions produce a damping effect which remains finite for long wavelengths. The effect of electron-electron collisions vanishes in this limit. The absorption of transverse radiation is also considered; calculations for the electron-ion plasma are in essential agreement with the recent work of Dawson and Oberman. The results for the absorptive part of the conductivity tensor for long-wavelength electromagnetic waves in a plasma where the phase velocity ω/k is much greater than the rms particle velocity is for the electron-ion plasma:

$$4\pi\,\mathrm{Im}\sigma_{ij}(\mathbf{k},\omega)=\frac{\Omega_p}{6\sqrt{2}\pi^{3/2}}\frac{\Omega_p^2}{\omega^2}\frac{k_D^3}{n}\ln\left(\frac{C_a(\omega)}{\beta\hbar\omega}\right)\delta_{ij},$$

where $\Omega_p^2=4\pi e^2nm^{-1}$, $k_D^2=4\pi e^2n\beta$, and $\beta=(kT)^{-1}$. The effects of dynamic screening are entirely contained in definite integral $C_a(\omega)$ which is numerically evaluated. The calculations are valid for temperatures and densities which satisfy the inequalities:

$$(4\pi e^2n/m)^{3/2}(\hbar/kT)^3\ll(4\pi e^2n/kT)^{3/2}n^{-1}\ll(4\pi e^2n/m)^{1/2}(\hbar/kT)\ll1.$$

Reading from left to right these inequalities justify the use of Boltzmann statistics, the Born approximation, and the neglect of wave mechanical interference effects. The weak-coupling approximation is justified by $(4\pi e^2n/kT)^{3/2}n^{-1}\ll1$. These restrictions are satisfied, for example, if $T>10^6$ °K and $n<10^{20}$ particles/cm^3. For these hot plasmas a natural short-wavelength cutoff appears at roughly the thermal de Broglie wavelength. Electrons and ions are found to produce comparable screening effects. To illustrate the application of these techniques to degenerate, low-temperature systems, the absorption process in a high-density electron gas is briefly considered.

I. INTRODUCTION

THIS paper deals mainly with the damping of electromagnetic waves in uniform, weakly interacting, fully ionized plasmas near equilibrium in the absence of steady external magnetic fields. We are primarily interested in hot, dilute electron-ion plasmas, although we also briefly consider a cold, dense degenerate electron gas.

We regard macroscopic electromagnetic plane waves of a given frequency and wave number $(\mathbf{k},\omega)$ as coherent superpositions of quantized photons or plasmons with the same $\mathbf{k}$ and ω. If the amplitude of the wave is sufficiently small, nonlinear interactions among these excitations can be neglected, and the damping rate of the wave is just the quantum-mechanical rate of absorption minus the rate of emission of the quantized excitations. These quantum processes are represented by Feynman diagrams and the rates are calculated by propagator techniques.

The rate of damping γ and the frequency dispersion relation for the electromagnetic waves are very simply related to the real and imaginary parts of the local tensor conductivity of the system, $\sigma_{ij}(\mathbf{k},\omega)$. We present a complete many-particle perturbation theory for σ_{ij} which includes longitudinal and transverse collective effects. We then calculate the exact two-particle collision contributions to σ_{ij}, taking into account the dynamic screening of the interaction. For the hot plasmas considered here, with $kT\gg me^4/\hbar^2$, a natural short-wavelength cutoff appears.

We find[1] that for long-wavelength longitudinal waves the main absorption mechanism in the cases mentioned above is the two-particle collision process and *not* the one-particle, or Landau damping, process. As a consequence, it becomes clear that the self-consistent field approximation and the equivalent random phase approximation are both inadequate for computing the damping rate of plasma oscillations.[2] The electron-ion plasma provides a striking illustration of the importance of the two-particle collision damping process: In the limit of infinite wavelength the Landau damping rate vanishes exponentially but the collision damping rate remains constant. For the electron gas in both the

* Present address: Hughes Research Laboratories, Malibu, California.

[1] D. F. DuBois, V. Gilinsky, and M. G. Kivelson, Phys. Rev. Letters 8, 419 (1962).

[2] There are many papers on the application of the self-consistent field approximation (Vlasov-Landau equation) to plasmons. For a recent review see V. L. Klimontovich and V. P. Silin, Soviet Phys.—Uspekhi 3, 84 (1960). The random phase approximation is applied to the damping of plasmons in a recent paper by D. Pines and J. R. Schrieffer, Phys. Rev. 125, 804 (1962).

classical and quantum[3] cases the collision damping vanishes like the inverse square of the wavelength in the long-wavelength limit, but is still considerably larger than Landau damping for wavelengths much greater than the Debye wavelength. It is then apparent that for collision damping, unlike Landau damping, the presence of discrete ions has an important effect.

For a wide range of temperatures and densities the most important role of the Landau damping process for uniform plasmas in the absence of magnetic fields is to provide an upper limit on the wave numbers for which the plasma oscillation mode is well defined. For smaller wave numbers (longer wavelengths) plasma waves decay primarily through the collision process.

The qualitative importance of collision damping was pointed out long ago in the well-known work of Bohm and Gross.[4] They noted that since Landau damping was so small as $k \to 0$, collision effects would dominate in this limit. However, a complete calculation of this effect was not carried out and until recently subsequen- authors have tended to avoid detailed analysis of colt lision damping.

Our results for the transverse conductivity of a classical electron-ion plasma are in agreement with the results of Perel and Eliashberg[5] and with the results of Dawson and Oberman and Dawson, Oberman, and Ron.[6]

Our methods are based on the recent developments in quantum-statistical mechanics which employ the powerful methods of quantum field theory.[7,8] We have arranged the paper in such a way that the reader who is primarily interested in results may go directly to Sec. III and then to Sec. VI, which can be read independently provided the rules for calculation given there are accepted.

In Sec. II we list the field operator notation for the problem of a system of several species of charged particles interacting via the static Coulomb potential and the transverse radiation field. Throughout this paper we consider only the nonrelativistic limit, in which it is convenient to work with a noncovariant formalism.

In Sec. III we outline the theory of electromagnetic waves in a dispersive medium. The frequency and damping of waves in a medium can be determined entirely from the *local* conductivities.

In Sec. IV the calculation of the retarded current commutator by a diagram expansion plus analytic continuation method, developed by several authors,[5,7] is discussed. The theory of the effective screened longitudinal interaction propagator and the propagator for photons in the medium is given. This enables us to connect the local conductivities to the calculation of proper polarization parts in the medium. A brief discussion of the results of the random phase approximation as obtained in our formalism is also given here.

In Sec. V the general features of the calculation of absorptive parts of diagrams are discussed. This approach,[9] which leans heavily on the dispersion relations obeyed by the various functions in the theory, enables us to use an open-diagram expansion technique for the calculation of absorptive parts which is simpler and as general as the closed-diagram techniques discussed in Sec. IV. The open-diagram approach has an additional intuitive advantage in that it essentially reduces the calculation to the form of the "golden rule" for transition probabilities.

Section VI is concerned with the application of these rules to the calculation of conductivities in the classical limit. The results described above are obtained here and their limits of validity are discussed. The inclusion of dynamic screening effects is carried out here and the results of numerical calculations are presented.

In Sec. VII we consider the absorption processes in a degenerate electron gas. The work of Tzoar and Klein[10] is discussed here. They considered the absorption of a photon into a final state of a pair plus a plasmon, but they neglected to cut off the possible plasmon momenta at the upper value k_c at which the plasmon energy, in lowest order, merges with the continuum of pair states. In the high-density limit for which a perturbation theory is valid, the introduction of a cutoff reduces the resonant effect which they predicted by such a large factor that it seems probable that the resonance would be lost in the continuum of two-pair final states.

Finally, in Sec. VIII we conclude with some comments about our results and possible extensions of this work.

II. FUNDAMENTAL EQUATIONS

In the notation of second quantization the Hamiltonian operator for a system of several interacting species of charged fermions with masses M_ν and charges eZ_ν can be written as

$$H = H_e + H_r + H_1, \tag{2.1}$$

[3] D. F. DuBois, Ann. Phys. (N. Y.) **8**, 24 (1959).

[4] D. Bohm and E. P. Gross, Phys. Rev. **72**, 1851 (1949). It has come to our attention that the importance of higher-order terms has been considered recently for the case of an electron gas by Ichikawa [V. H. Ichikawa, Progr. Theoret. Phys. (Kyoto) **24**, 1083 (1960)]. A similar calculation has recently been reported by Willis [C. R. Willis, Phys. Fluids **5**, 219 (1962)], who obtains a somewhat different result. These calculations are based on a truncation approximation in the hierarchy of kinetic equations and lead to results qualitatively in agreement with our exact result. Neither of these authors obtains the correct logarithmic factor in his result.

[5] V. I. Perel and G. M. Eliashberg, J. Exptl. Theoret. Phys. (U.S.S.R.) **41**, 886 (1961).

[6] J. Dawson and C. Oberman, Phys. Fluids **5**, 517 (1962); J. Dawson, C. Oberman, and A. Ron, *ibid.* (to be published).

[7] A. A. Abrikosov, L. P. Gor'kov, and I. E. Dzyaloshinskii, J. Exptl. Theoret. Phys. (U.S.S.R.) **36**, 900 (1959) [translation: Soviet Phys.—JETP **9**, 636 (1959)].

[8] P. C. Martin and J. Schwinger, Phys. Rev. **115**, 1342 (1959).

[9] J. S. Langer, Phys. Rev. **124**, 997 (1961).

[10] N. Tzoar and A. Klein, Phys. Rev. **124**, 1297 (1961).

where[11]

$$H_e=-\sum_\nu \frac{1}{2M_\nu}\int d^3x\,\psi_\nu^\dagger(\mathbf{x},t)\nabla^2\psi_\nu(\mathbf{x},t), \tag{2.2}$$

$$H_r=\frac{1}{8\pi}\int d^3x\,[\mathbf{E}_T^2(\mathbf{x},t)+\mathbf{B}^2(\mathbf{x},t)], \tag{2.3}$$

$$\begin{aligned}H_1=&\tfrac{1}{2}\int d^3x\int d^3x'\,\rho(\mathbf{x}')v(\mathbf{x}-\mathbf{x}')\rho(\mathbf{x}')\\&-\tfrac{1}{2}\sum_\nu e^2Z_\nu^2N_\nu v(0)-\frac{1}{c}\int d^3x\,\mathbf{J}(\mathbf{x},t)\cdot\mathbf{A}(\mathbf{x},t)\\&-\tfrac{1}{2}\sum_\nu\frac{Z_\nu e}{M_\nu c^2}\int d^3x\,\rho_\nu(\mathbf{x},t)\mathbf{A}^2(\mathbf{x},t).\end{aligned} \tag{2.4}$$

Here $\psi_\nu(\mathbf{x},t)$ is the field operator in the Heisenberg picture for a fermion of species ν with mass M_ν. These field operators obey anticommutation rules for equal time arguments:

$$\begin{aligned}[\psi_\nu(\mathbf{x},t),\psi_{\nu'}^\dagger(\mathbf{x}',t)]_+&=\delta_{\nu\nu'}\delta^3(\mathbf{x}-\mathbf{x}'),\\ [\psi_\nu(\mathbf{x},t),\psi_\nu(\mathbf{x}',t)]_+&=[\psi_\nu^\dagger(\mathbf{x},t),\psi_\nu^\dagger(\mathbf{x}',t)]_+=0.\end{aligned} \tag{2.5}$$

H_e is the kinetic energy of the particle fields and H_r is the energy in the electromagnetic field. Operators for different species commute.

We use the Coulomb gauge[12] in which the vector potential field operator $\mathbf{A}(\mathbf{x},t)$ obeys the transversality condition

$$\nabla\cdot\mathbf{A}(\mathbf{x},t)=0. \tag{2.6}$$

The electromagnetic field operators obey equal time commutation relations of the form

$$\begin{aligned}&\frac{1}{4\pi c^2}[A_i(\mathbf{x},t),A_j(\mathbf{x}',t)]_-\\&\quad=-i\left[\delta_{ij}\delta^3(x-x')+\frac{1}{4\pi}\nabla_i\nabla_j\left(\frac{1}{|\mathbf{x}-\mathbf{x}'|}\right)\right].\end{aligned} \tag{2.7}$$

The electric and magnetic field operators $\mathbf{E}_T$ and $\mathbf{B}$ are obtained from $\mathbf{A}$ by the usual relations

$$\mathbf{E}_T=-(1/c)(d\mathbf{A}/dt),\quad \mathbf{B}=\nabla\times\mathbf{A}. \tag{2.8}$$

The longitudinal or electrostatic part of the electric field, $\mathbf{E}_L$ is contained in the static Coulomb interaction which is the first term in Eq. (2.4) with

$$v(|\mathbf{x}-\mathbf{x}'|)=(1/|\mathbf{x}-\mathbf{x}'|). \tag{2.9}$$

The total electric field operator is then

$$\mathbf{E}=\mathbf{E}_L+\mathbf{E}_T, \tag{2.10}$$

where the electrostatic part is

$$\mathbf{E}_L(\mathbf{x},t)=-\int d^3x'\,\nabla v(\mathbf{x}-\mathbf{x}')\rho(\mathbf{x}',t). \tag{2.10a}$$

The second term in Eq. (2.4) makes the usual subtraction of the electrostatic self-energy and the last term is the interaction of the particles with the transverse electromagnetic field. The charge density operator $\rho(\mathbf{x},t)$ is

$$\rho(\mathbf{x},t)=\sum_\nu\rho_\nu(\mathbf{x},t)=\sum_\nu eZ_\nu\psi_\nu^\dagger(\mathbf{x},t)\psi_\nu(\mathbf{x},t), \tag{2.11}$$

and N_ν, the total number operator for particles of species ν, is given by

$$Z_\nu eN_\nu=Z_\nu e\int d^3x\,\psi_\nu^\dagger(\mathbf{x},t)\psi_\nu(\mathbf{x},t)=\int d^3x\,\rho_\nu(\mathbf{x},t). \tag{2.12}$$

$\mathbf{J}(\mathbf{x},t)$ is the total current operator in the electromagnetic field related to the field-free current operator $\mathbf{j}(\mathbf{x},t)$ by

$$\mathbf{J}(\mathbf{x},t)=\mathbf{j}(\mathbf{x},t)-\sum_\nu(eZ_\nu/M_\nu c)\rho_\nu(\mathbf{x},t)\mathbf{A}(\mathbf{x},t), \tag{2.13}$$

where

$$\begin{aligned}\mathbf{j}(\mathbf{x},t)=&\sum_\nu(eZ_\nu/2M_\nu i)\\&\times\{\psi_\nu^\dagger(\mathbf{x},t)\nabla\psi_\nu(\mathbf{x},t)-[\nabla\psi_\nu^\dagger(\mathbf{x},t)]\psi_\nu(\mathbf{x},t)\}.\end{aligned} \tag{2.14}$$

Conservation of charge is ensured by the continuity equation

$$\dot\rho(\mathbf{x},t)=i[H,\rho(\mathbf{x},t)]_-=-\nabla\cdot\mathbf{J}(\mathbf{x},t). \tag{2.15}$$

In the nonrelativistic limit which we consider here, the noncovariant separation of the Coulomb interaction is convenient since when $\langle v\rangle\ll c$, where $\langle v\rangle$ is the rms velocity, we can usually neglect the interactions through the transverse electromagnetic field.

We are interested here in two cases:

(i) *The electron gas*—where $\nu=1$, $M_1=m$, $Z_1=-1$. The charge neutrality of the system is maintained by smearing out the positive charge into a uniform background whose only effect is to maintain the average total charge density at zero.

(ii) *The electron-ion plasma*—where $\nu=1$, 2, and

$$M_1=m,\quad M_2=M;\quad Z_1=-1,\quad Z_2=Z.$$

Here charge neutrality is again imposed by the condition that the average total charge be zero.

III. ELECTROMAGNETIC WAVES IN A MEDIUM

In the absence of external sources, electromagnetic waves may exist in a many-particle medium. Because of the absorptive properties of the medium, however, such waves are generally damped in time, unlike electromagnetic waves in a vacuum. Suppose the external sources are turned off at $t=0$. What is the subsequent behavior of the field in the medium?

[11] Except in Sec. VI we use units in which $\hbar=1$.

[12] L. Schiff, *Quantum Mechanics* (McGraw-Hill Book Company, Inc., New York, 1949); W. Heitler, *The Quantum Theory of Radiation* (Oxford University Press, New York, 1954).

Because of the relaxation effects in a many-particle medium we must know the history of the local field in the medium for values $t<0$ to solve this initial value problem. We restrict our considerations to systems in which the total electric field in the medium $E(\mathbf{x},t)$ (i.e., the external field plus the induced fields) is linearly related to the field due to the external sources alone $E^0(\mathbf{x},t)$. For a uniform system we can write this relationship as

$$E_i^0(\mathbf{x},t)=\int d^3x'\int_{-\infty}^{\infty}dt'\ \epsilon_{ij}(\mathbf{x}-\mathbf{x}',t-t')E_j(\mathbf{x}',t'), \quad (3.1)$$

where ϵ_{ij} is called the dielectric tensor of the medium. The requirement of causality[13] demands that ϵ_{ij} vanish if $t<t'$. Such a nonlocal relationship in space and time is necessary to take into account that (i) currents and charges induced at time t' relax toward equilibrium with some characteristic time and thus can affect the field at some later time and (ii) spatially inhomogeneous charge and current distributions are removed by transport of charge so that the distribution at $\mathbf{x}'$ can affect the field at $\mathbf{x}$.

The electrodynamics of a many-particle medium, based on the dielectric tensor and the related local conductivity tensor $\sigma_{ij}(\mathbf{x}-\mathbf{x}',t-t')$ is discussed elsewhere,[8,14] The four-dimensional Fourier transforms of the longitudinal and transverse parts of these tensors are related as follows[15]:

$$\begin{aligned}\epsilon_L(\mathbf{k},\omega)&=1+4\pi\sigma_L(\mathbf{k},\omega)/\omega,\\ \epsilon_T(\mathbf{k},\omega)&=1+4\pi\omega\sigma_T(\mathbf{k},\omega)/(\omega^2-c^2k^2).\end{aligned} \quad (3.2)$$

The external conductivity tensor which relates the average current in the medium to the external electric field is defined in terms of the above quantities as

$$\sigma_{ij}{}^0=(k_ik_j/k^2)\sigma_L{}^0+(\delta_{ij}-k_ik_j/k^2)\sigma_T{}^0, \quad (3.3)$$

where

$$\begin{aligned}\sigma_L{}^0&=\sigma_L/\epsilon_L,\\ \sigma_T{}^0&=\sigma_T/\epsilon_T.\end{aligned}$$

This tensor is related to the transform of the averaged retarded current commutator

$$\Pi_{ij}{}^+(\mathbf{x}-\mathbf{x}',t-t')=i\eta(t-t')\langle[J_i(\mathbf{x},t),J_j(\mathbf{x}',t')]_-\rangle_0, \quad (3.4)$$

where $\eta(t-t')$ is a step function requiring that $t>t'$, and the current operator $J_i(\mathbf{x},t)$ is defined in Eqs. (2.13) and (2.14). The average implied by the bracket is with respect to the equilibrium ensemble. The fundamental equation[8] connecting $\sigma_{ij}{}^0$ to the transform of $\Pi_{ij}{}^+$ is

$$\omega\sigma_{ij}{}^0(\mathbf{k},\omega)=\Pi_{ij}{}^+(\mathbf{k},\omega)-\delta_{ij}\Omega_p{}^2/4\pi, \quad (3.5)$$

where $\Omega_p{}^2=4\pi e^2\sum_\nu Z_\nu{}^2n_\nu/M_\nu$ with n_ν the average equilibrium number density of species ν. Similar relations have been derived in the past by several authors.[16] $\Pi_{ij}{}^+$ then provides complete information concerning the linear electromagnetic properties of the many-particle system and provides the connection between the macroscopic phenomena and the microscopic theory. In the next section we review the calculation of $\Pi_{ij}{}^+$ by means of a diagrammatic many-particle perturbation theory. First, we must establish the connection of σ_L and σ_T with the frequency and damping of electromagnetic waves in the plasma.

The electromagnetic response of the system is determined by the zeros of the dielectric constants. The case of greatest interest for wave propagation is that in which $\epsilon_L{}^{-1}(\mathbf{k},\omega)$ and $\epsilon_T{}^{-1}(\mathbf{k},\omega)$ have one or two large resonances which dominate the spectrum.

When the electric fields are well-behaved functions, the resonant frequencies are determined by the relations,

$$\mathrm{Re}\epsilon_L(\mathbf{k},\omega_L)=1+4\pi\ \mathrm{Re}\sigma_L(\mathbf{k},\omega_L)/\omega_L=0, \quad (3.6)$$

and

$$\mathrm{Re}\epsilon_T(\mathbf{k},\omega_T)=1+4\pi\omega_T\ \mathrm{Re}\sigma_T(\mathbf{k},\omega_T)/(\omega_T{}^2-c^2k^2)=0, \quad (3.7)$$

where we have used Eq. (3.2).

We can write in the neighborhood of these resonances

$$\epsilon_L{}^{-1}(\mathbf{k},\omega)=\frac{\omega_L}{2}\frac{Z_L}{\omega-\omega_L+\frac{1}{2}i\gamma_L}, \quad (3.8)$$

$$\epsilon_T{}^{-1}(\mathbf{k},\omega)=\frac{\omega_T{}^2-c^2k^2}{2\omega_T}\frac{Z_T}{\omega-\omega_T+\frac{1}{2}i\gamma_T}, \quad (3.9)$$

where

$$Z_L{}^{-1}=\frac{\omega_L}{2}\frac{\partial}{\partial\omega}\left[\frac{4\pi\ \mathrm{Re}\sigma_L(\mathbf{k},\omega)}{\omega}\right]_{\omega=\omega_L}, \quad (3.10)$$

$$\gamma_L(\mathbf{k})=Z_L4\pi\ \mathrm{Im}\sigma_L(\mathbf{k},\omega_L),$$

and

$$Z_T{}^{-1}=1+\frac{\partial}{\partial\omega^2}[4\pi\omega\ \mathrm{Re}\sigma_T(\mathbf{k},\omega)]_{\omega=\omega_T}, \quad (3.11)$$

$$\gamma_T(\mathbf{k})=Z_T4\pi\ \mathrm{Im}\sigma_T(\mathbf{k},\omega_T).$$

The conditions for validity of these formulas are the smoothness of the Fourier transforms of the electric

[13] Since the external field $E_i{}^0$ is the cause which produces the internal field E_i, the causality requirement on ϵ_{ij} is not immediately obvious. However, note that $E_i{}^0(t)$ is the difference between the total field at t and the induced field. The latter is causally related to $E_j(t')$. Thus, $\epsilon_{ij}(t-t')$ is causal except for a delta function at $t=t'$.

[14] A detailed discussion of the electrodynamics of many-particle systems is contained in D. F. DuBois, V. Gilinsky, and M. G. Kivelson, RAND Corporation, Report RM-3224-AEC, August, 1962 (unpublished), see especially Appendix A. The reader should be cautioned that the arguments of the logarithms in the results for the conductivity presented in Sec. VI of this report are incorrect because two diagrams have been overlooked. These diagrams correspond to the lower diagrams in Fig. 10 of this paper.

[15] Note that our definition of σ_{ij} differs by a factor of i from the usual one. Thus, $\mathrm{Re}\sigma_L$ is related to the polarizability while $\mathrm{Im}\sigma_L$ is the usual electric conductivity. We use this convention so that absorptive parts are always related to the imaginary parts of quantities in this paper.

[16] See, for example, reference 7 and P. A. Wolff, Phys. Rev. **116**, 554 (1959).

field in the neighborhood of the resonances and the conditions

$$\gamma_L(\mathbf{k})/\omega_L(\mathbf{k})\ll 1 \quad \text{and} \quad \gamma_T(\mathbf{k})/\omega_T(\mathbf{k})\ll 1, \tag{3.12}$$

which require the resonances to be sharp. If there are several resonances, then the expressions for $\mathbf{E}_L$ and $\mathbf{E}_T$ have a sum of terms, one for each resonance.

If we examine the time dependence implied by Eqs. (3.4) and (3.5) we find[17]

$$\mathbf{E}_L(\mathbf{k},t)\sim\exp(-i\omega_L t-\tfrac{1}{2}\gamma_L t), \tag{3.13}$$

$$\mathbf{E}_T(\mathbf{k},t)\sim\exp(-i\omega_T t-\tfrac{1}{2}\gamma_T t). \tag{3.14}$$

There are no longitudinal waves in the vacuum (i.e., $\sigma_L=0$). In a plasma there may be several longitudinal waves, the most important of which are the plasma oscillations. Equations (3.6) and (3.10) give us a generalized way of determining the frequency and damping of such oscillations in terms of the conductivity for which we will develop a power series expansion in the next section. Transverse waves do exist in vacuum as evidenced by the fact that Eq. (3.7) has the solution $\omega^2=c^2k^2$ *in the limit* as $\sigma_T\to 0$. In a medium Eqs. (3.7) and (3.11) allow us to calculate the frequency shift and damping of transverse waves.

In the next section we present sum-rule criteria for determining whether these resonances actually dominate the entire spectrum.

IV. MICROSCOPIC THEORY: PROPAGATORS AND DIAGRAMMATIC PERTURBATION THEORY

Spectral Properties

It is shown elsewhere[8,14] that the external conductivity tensor $\sigma_{ij}^0(\mathbf{k},\omega)$ can be calculated from the averaged retarded current commutator given in Eq. (3.4). The equilibrium average denoted there is most conveniently taken with respect to the grand canonical distribution:

$$\varrho=e^{\beta\Omega}e^{-\beta(H-\mu\cdot N)}, \qquad e^{\beta\Omega}=\mathrm{Tr}[e^{-\beta(H-\mu\cdot N)}], \tag{4.1}$$

$$\langle\cdots\rangle_0=\mathrm{Tr}[\varrho\cdots]. \tag{4.2}$$

Here $\beta=(kT)^{-1}$ is the reciprocal of the equilibrium temperature and we use the notation $\mu\cdot N=\sum_\nu \mu_\nu N_\nu$. The chemical potential of species ν, μ_ν, is chosen so that the average number of particles of species ν, which we denote by

$$\bar{N}_\nu=\langle N_\nu\rangle_0, \tag{4.3}$$

is the observable number. In addition, the μ_ν are related by the condition of charge neutrality

$$\sum_\nu Z_\nu\bar{N}_\nu=0. \tag{4.4}$$

Our main task in this section is to evaluate the function Π_{ij}^+. Perturbation techniques have recently been developed, particularly by several Russian authors,[5,7] which involve the calculation of certain thermodynamic Green's functions from which the retarded commutator functions are calculated by an analytic continuation procedure. In our formulation of this method, we relate the retarded commutator functions to imaginary-temperature Green's functions or propagators as done, for instance, by Martin and Schwinger.[8] These imaginary-temperature propagators, which we distinguish with a tilde, are defined as

$$\tilde{\Pi}_{ij}(1,2)=i\frac{\mathrm{Tr}[e^{-i\tau(H-\mu\cdot N)}TJ_i(1)J_j(2)]}{\mathrm{Tr}[e^{-i\tau(H-\mu\cdot N)}]} \tag{4.5}$$

in the interval $|t_1-t_2|\leq\tau$. Here τ is an imaginary temperature variable (actually, τ must have a small negative imaginary part to insure convergence) and T is Wick's well-known, time-ordering operator.

$$\begin{aligned} TJ_i(1)J_j(2)&=J_i(1)J_j(2), \quad t_1>t_2\\ &=J_j(2)J_i(1), \quad t_1\leq t_2. \end{aligned} \tag{4.6}$$

The function $\tilde{\Pi}_{ij}(1,2)$ is mathematically convenient because it obeys periodic boundary conditions in time,

$$\tilde{\Pi}_{ij}(\mathbf{x}_1,\mathbf{x}_2;t_1-t_2-\tau)=\tilde{\Pi}_{ij}(\mathbf{x}_1,\mathbf{x}_2;t_1-t_2), \tag{4.7}$$

as may be demonstrated from the invariance of the trace under cyclic permutation.[8] The time dependence of $\tilde{\Pi}_{ij}$ can, therefore, be represented by a Fourier series while the spatial dependence is again represented by a Fourier integral

$$\tilde{\Pi}_{ij}(1,2)=\int\frac{d^3k}{(2\pi)^3}\frac{1}{\tau}\times\sum_{k_0}\tilde{\Pi}_{ij}(\mathbf{k},k_0)e^{i\mathbf{k}\cdot(\mathbf{x}_1-\mathbf{x}_2)}e^{-ik_0(t_1-t_2)}, \tag{4.8}$$

where $k_0=\pi\kappa/\tau$, κ is an even integer, and

$$\tilde{\Pi}_{ij}(\mathbf{k},k_0)=\frac{1}{2}\int d^3(x_1-x_2)\int_{-\tau}^{\tau}d(t_1-t_2)\times\tilde{\Pi}_{ij}(1,2)e^{-i\mathbf{k}\cdot(\mathbf{x}_1-\mathbf{x}_2)}e^{ik_0(t_1-t_2)}. \tag{4.9}$$

Now Π_{ij}^+ can be calculated from $\tilde{\Pi}_{ij}$ by an analytic continuation procedure which is most easily described in terms of the spectral representations of their Fourier coefficients. Using a complete set of states $|n\rangle$ which diagonalizes the operators H, N, and P (the total momentum) and the Heisenberg equations of motion,

[17] The time dependence can be analyzed in an alternate way. In computing the transform of the electric field one notes that there are poles in the lower half ω plane where $\epsilon_L=0$ or $\epsilon_T=0$, respectively. Since ϵ_L or ϵ_T have, in general, a branch discontinuity along the real ϵ axis it follows that these poles lie on the next Reimann sheets of these functions. If we deform the contour of integration over ω into the next sheet in such a way as to encircle the poles then the contributions from the poles are of the form of Eq. (3.13) or (3.14) while the remaining contributions are of order γ_L/ω_L or γ_T/ω_T, respectively.

it follows by well-known techniques that we may write

$$\Pi_{ij}^{+}(\mathbf{k},\omega)=\int_{-\infty}^{\infty}\frac{d\omega'}{\pi}\frac{1}{\omega-\omega'+i\epsilon}A_{ij}^{(\beta)}(\mathbf{k},\omega'), \quad (4.10)$$

$$\tilde{\Pi}_{ij}(\mathbf{k},k_0)=\int_{-\infty}^{\infty}\frac{d\omega'}{\pi}\frac{1}{k_0-\omega'}A_{ij}^{(i\tau)}(\mathbf{k},\omega'), \quad (4.11)$$

where

$$A_{ij}^{(\beta)}(\mathbf{k},\omega)=\pi\sum_{nm}\varrho_n^{(\beta)}\langle n|J_i(0)|m\rangle \times\langle m|J_j(0)|n\rangle(1-e^{-\beta\omega}) \quad (4.12)$$
$$\delta(\omega-E_m+E_n)(2\pi)^3\delta^3(\mathbf{k}-\mathbf{P}_m+\mathbf{P}_n),$$

and where

$$\varrho_n^{(\beta)}=e^{\beta\Omega}\,e^{-\beta(E_n-\mu\cdot N_n)}$$
$$e^{-\beta\Omega}=\mathrm{Tr}[e^{-\beta(H-\mu N)}]=\sum_n e^{-\beta(E_n-\mu\cdot N_n)}. \quad (4.13)$$

It is apparent then that Π_{ij}^{+} can be obtained from $\tilde{\Pi}_{ij}$ by continuing the discrete variable k_0 to continuous values in the upper half plane $k_0\rightarrow\omega+i\epsilon$ and simultaneously setting $i\tau=\beta$. The mathematical details of this procedure are given in several references.[7,8]

In addition to making the analytic continuation procedure very explicit, the spectral representations are a distinct aid in simplifying calculations as is seen in Sec. V.

Perturbation Theory: Closed Diagrams

The main advantage of using the imaginary temperature functions $\tilde{\Pi}_{ij}$, with their periodic boundary conditions in time, is that they can be calculated in a systematic power series in the interaction strength similar to the diagrammatic perturbation theory of Feynman in vacuum quantum electrodynamics. The retarded function Π_{ij}^{+} or the real-temperature Green's functions cannot be so treated except in special cases.[18]

Using well-known methods,[19] we can write $\tilde{\Pi}_{ij}(1,2)$ in the form

$$\tilde{\Pi}_{ij}(1,2)=i\frac{\mathrm{Tr}[\varrho^0(i\tau)TU(\tau,0)\mathcal{J}_i(1)\mathcal{J}_j(2)]}{\mathrm{Tr}[\varrho^0(i\tau)U(\tau,0)]}, \quad (4.14)$$

where

$$\varrho^0(i\tau)=\exp(-i\tau\bar{H}_0)/\mathrm{Tr}[\exp(-i\tau\bar{H}_0)] \quad (4.15)$$

is the ensemble density for the interaction free system at imaginary temperature, $U(\tau,0)=\exp(i\tau\bar{H}_0)\exp(-i\tau\bar{H})$, and $\mathcal{J}_i(1)$ is the current operator in the interaction picture. Thus, by going to the interaction picture we have reduced the statistical averaging to the computation of averages in the interaction free ensemble. This allows us to make use of the algebraic theorem of Wick to expand $\tilde{\Pi}_{ij}(\mathbf{k},\omega)$ in powers of the interaction strength (i.e., in powers of H_1) and we are subsequently led to a form of diagrammatic perturbation theory.[20]

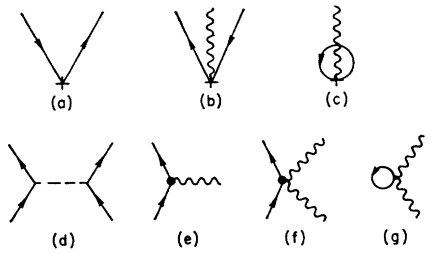

FIG. 1. Basic elements of diagrams. (a) Simple current-measuring vertex; (b) quadratic current-measuring vertex; (c) quadratic counter term in current-measuring vertex; (d) static Coulomb interaction; (e) simple transverse photon interaction vertex; (f) quadratic transverse photon interaction vertex; (g) quadratic counter term.

The prescription for calculating the Fourier coefficient $\tilde{\Pi}_{ij}(\mathbf{k},k_0)$ is as follows: We draw all connected diagrams leading from a current measuring vertex (denoted by a cross) with incoming momentum $\mathbf{k}$ and energy k_0, and ending with another current measuring vertex with outgoing momentum $\mathbf{k}$ and energy k_0. There are two types of current-measuring vertices corresponding to the two terms in the expression (2.13) for the current operator. The first is a simple vertex as in Fig. 1(a) and the second is a vertex involving the additional emission or absorption of a photon as in Fig. 1(b). The order of the diagrams is classified according to the number of static Coulomb interactions (dashed lines) and the number of transverse photon (wiggly lines) interactions [see Figs. 1(d), (e), and (f)]. Additional quadratic vertices shown in Figs. 1(c) and (g) arise from the quadratic particle-field interaction. These diagrams represent the interaction of the photons with the average charge density of the medium (represented by the closed loop) through the counter term $(\mathbf{A}^2/c^2)\sum_\nu e^2Z_\nu^2n_\nu/M_\nu$, which, in turn, is necessary to maintain gauge invariance.

Diagrams to first order in both longitudinal and transverse interactions are shown in Fig. 2, higher-order diagrams in the Coulomb interaction in Fig. 3. The meaning of these diagrams is clear. A measurement of the $\mathbf{k}$, k_0 Fourier component of the current is made which excites the system from equilibrium producing a particle-hole pair. (Particles are denoted by upward solid lines and holes by downward solid lines.) That is, a fermion in the equilibrium medium is scattered out of a state leaving the state underpopulated by one, relative to the equilibrium distribution, thus creating a hole in this state. The state into which the fermion is scat-

[18] At absolute zero temperature there exists a similar expansion for the real-temperature Green's function provided the Fermi surface for the interacting system coincides with that of the non-interacting system. See, for example, J. M. Luttinger and J. C. Ward, Phys. Rev. 118, 1417 (1960).

[19] S. S. Schweber, *An Introduction to Relativistic Quantum Field Theory* (Row, Peterson & Company, Evanston, Illinois, 1961).

[20] Developments similar to this are carried out in reference 6 and by T. Matsubara, Progr. Theoret. Phys. (Kyoto) 14, 351 (1955). Note that diagrams representing the interaction of particles with the average charge density of the medium are not included in our work since we are considering an electrically neutral system.

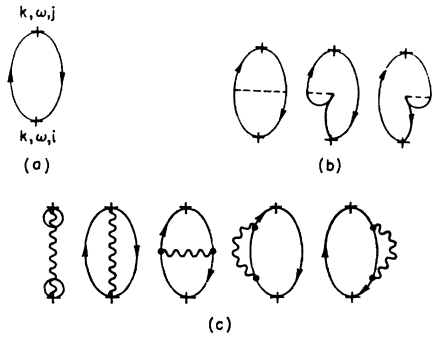

FIG. 2. Diagrams to first order for $\tilde{\Pi}_{ij}(\mathbf{k},\omega)$. (a) Zero-order diagram; (b) first-order diagrams in longitudinal Coulomb interaction; (c) first-order diagrams in transverse interaction.

tered is now overpopulated by one and is represented by the particle line. The particle and hole, thus excited, interact with each other and with the equilibrium medium (producing additional pairs) until the system is deexcited by another current measurement. In a two-component ion-electron plasma we represent the electrons by thin solid lines and the ions by heavy solid lines. The additional diagrams which arise in this case are obtained by replacing electron closed loops in the diagrams given by ion closed loops in all possible combinations.

The contribution to $4\pi i\tilde{\Pi}_{ij}(\mathbf{k},k_0)$ from each diagram is calculated by writing:

(1) A factor $\tilde{G}_\nu{}^0(\mathbf{p},p_0)$ for each fermion line of mass M_ν, momentum $\mathbf{p}$, and energy p_0, where

$$\tilde{G}_\nu{}^0(\mathbf{p},p_0)=i/(p_0-\xi_{\mathbf{p}}{}^\nu), \tag{4.16}$$

with

$$\xi_{\mathbf{p}}{}^\nu=(\mathbf{p}^2/2M_\nu)-\mu_\nu. \tag{4.17}$$

[For exchange loops such as those in Figs. 2(c) and 2(d) we need an additional convergence factor $e^{ip_0'+}$.]

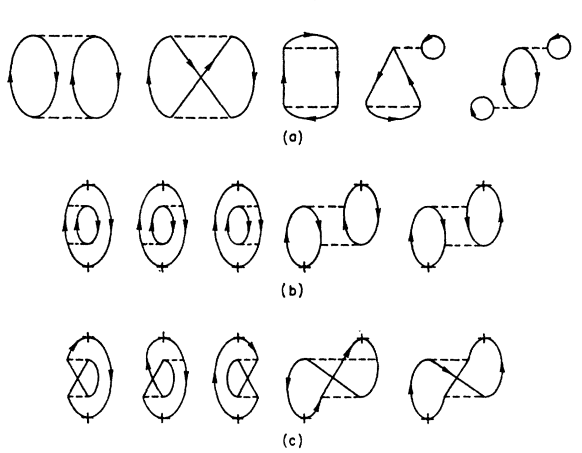

FIG. 3. Second-order diagrams. (a) Basic equilibrium diagrams from which diagrams for $\tilde{\Pi}_{ij}$ are obtained by inserting two current-measuring vertices in all topologically distinct ways; (b) diagrams for $\tilde{\Pi}_{ij}$ obtained from first of diagram (a); (c) diagrams for $\tilde{\Pi}_{ij}$ obtained from second of diagram (a).

(2) A factor

$$-ie^2Z_\nu Z_{\nu'}v(\mathbf{q})=-iZ_\nu Z_{\nu'}4\pi e^2/q^2 \tag{4.18}$$

for each static Coulomb line of momentum $\mathbf{q}$ connecting particle lines of charges Z_ν and $Z_{\nu'}$, respectively.

(3) A factor, $i\tilde{D}_{ij}{}^0$,

$$\tilde{D}_{ij}{}^0(\mathbf{k},k_0)=\frac{c^2(\delta_{ij}-k_ik_j/k^2)}{k_0{}^2-k^2c^2} \tag{4.19}$$

for each transverse photon line of momentum $\mathbf{k}$, energy k_0.

(4a) A current factor for each simple current measuring vertex or single photon-fermion vertex

$$-i(4\pi)^{1/2}(Z_\nu e/2M_\nu c)(p_j+p_j'), \tag{4.20}$$

where p_j is the momentum of the incoming fermion (of mass M_ν) and p_j' is the momentum of the outgoing fermion.

(4b) A factor for each simple charge density measuring vertex

$$-i(4\pi)^{1/2}Z_\nu e. \tag{4.21a}$$

(5) A factor for each double photon-fermion vertex

$$(\hat{e}\cdot\hat{e}')i4\pi e^2Z_\nu{}^2/M_\nu c^2. \tag{4.21b}$$

(6) A factor of (-1) for each closed fermion loop.

(7) Delta functions conserving energy and momentum at each vertex

$$-i(2\pi)^3\beta\delta^3(\mathbf{p}-\mathbf{p}'+\mathbf{q})\delta(p_0-p_0'+q_0), \tag{4.22}$$

where the energy delta function is a Kronecker delta.

(8) All internal momentum and energy variables are integrated and summed over according to the prescription

$$(i/\beta)\sum_{p_0}\int\frac{d^3p}{(2\pi)^3}, \tag{4.23}$$

where p_0 is summed over all values

$$p_0=i\pi\kappa/\beta, \tag{4.24}$$

and κ is an odd integer for fermions and an even integer for bosons.

Some comments are in order concerning these rules. In addition to the wave mechanical effects, the correct quantum statistics of the fermions and boson photons are built into the theory. Thus, exchange interactions between holes and particles and between holes and holes are included. These give a vanishingly small contribution in the extreme classical limit of high temperatures and low densities. This limit is discussed in Sec. VI.

The vertex factor of rule 4 arises from the $\mathbf{j}\cdot\mathbf{A}$ term in Eqs. (2.4) and (2.13), while the quadratic factor in rule 5 arises from the $eZ_\nu\rho_\nu\mathbf{A}^2/M_\nu c^2$ term. It is well known that if a relativistic Dirac theory for the particles is used there is only a linear vertex, the effect of the quadratic vertex coming from higher-order diagrams. The added complication in the present non-

relativistic treatment is compensated by the fact that the transverse interactions give rise to contributions of order $\langle v\rangle/c$ ($\langle v\rangle$ is the rms velocity) relative to the Coulomb contributions and can usually be neglected in the nonrelativistic region where $\langle v\rangle/c\ll 1$.

Note also that in the rules given above, we have already taken the limit $i\tau\to\beta$ which is part of the continuation procedure for going from $\tilde{\Pi}_{ij}$ to $\Pi_{ij}{}^{+}$. This is readily justified on closer inspection of the rules. We must still perform the analytic continuation which takes us from discrete k_0 to continuous ω.

Since this theory uses the grand canonical ensemble, a calculation is not complete unless the chemical potential μ for species ν is known to the order in the interactions to which the calculations are performed. In the present paper, since we are actually calculating the lowest order effects of the interactions, it turns out that we will need μ only to zeroth order:

$$\exp\beta\mu_\nu{}^0=n_\nu(2\pi\beta/M_\nu)^{3/2}. \tag{4.25}$$

Corrections to μ and, in fact, to all thermodynamic properties of the system can be calculated using the Green's function formalism. To calculate μ for the electron gas, one uses the condition that the average number of electrons per unit volume is n, and for the electron-ion case the added condition of charge neutrality. We refer the reader to the references for details of such calculations.[7,18]

Collective Effects

Longitudinal

The most important interaction effects in a plasma arise from the polarization of the many-particle medium by both longitudinal and transverse electromagnetic disturbances. The treatment of these collective effects insofar as they modify the longitudinal Coulomb interaction has been given in many papers[21–23] and in various contexts, so we only sketch the arguments here.

The propagator for the uncorrected Coulomb interaction, $v(\mathbf{k})=1/k^2$, is, of course, very divergent in the limit of small momentum transfers. It is well known that to obtain physically meaningful results $v(\mathbf{k})$ must be replaced by the screened interaction $\tilde{V}(\mathbf{k},k_0)$, where

$$\tilde{V}(\mathbf{k},k_0)=\frac{v(\mathbf{k})}{1+k^{-2}\tilde{Q}(\mathbf{k},k_0)}, \tag{4.26}$$

and $\tilde{Q}(\mathbf{k},k_0)$ is the proper polarization part. In lowest order we have

$$\tilde{Q}^0(\mathbf{k},k_0)=4\pi e^2\int\frac{d^3p}{(2\pi)^3}\frac{f(\xi_{\mathbf{p}+\mathbf{k}})-f(\xi_{\mathbf{p}})}{k_0-\xi_{\mathbf{p}+\mathbf{k}}+\xi_{\mathbf{p}}}, \tag{4.27}$$

with $f(\xi)=1/(1+e^{\beta\xi})$.

[21] M. Gell-Mann and K. A. Brueckner, Phys. Rev. **106**, 364 (1957).

[22] J. Hubbard, Proc. Roy. Soc. (London) **A240**, 539 (1957); **243**, 336 (1958).

[23] D. F. DuBois, Ann. Phys. (N. Y.) **7**, 174 (1959). The notation used here closely follows this reference.

It is instructive to write Eq. (4.34) as

$$\tilde{V}(\mathbf{k},k_0)=v(\mathbf{k})/\tilde{\epsilon}_L(\mathbf{k},k_0), \tag{4.28}$$

where

$$\tilde{\epsilon}_L(\mathbf{k},k_0)=1+k^{-2}\tilde{Q}(\mathbf{k},k_0) \tag{4.29}$$

is an effective dynamic longitudinal dielectric constant. If we analytically continue $\tilde{\epsilon}_L(\mathbf{k},k_0)$ to continuous values of $k_0=\omega+i\epsilon$ in the upper half-plane, the continuation is $\epsilon_L(\mathbf{k},\omega)$ the longitudinal dielectric constant defined in Sec. III.[14] From this it follows that the local conductivity is related to Q^{+} by

$$4\pi\sigma_L(\mathbf{k},\omega)=(\omega/k^2)Q^{+}(\mathbf{k},\omega). \tag{4.30}$$

This relation and Eqs. (3.6) and (3.10) allow us to compute the effects of many-particle interactions on the propagation of longitudinal waves in a plasma.

In our modified perturbation theory the corrected interaction lines are emitted or absorbed in quantized units. In the case where the resonance at the plasma frequency dominates, the propagator for each line is that for an elementary boson excitation which we identify as the plasmon. We may regard the long-wavelength macroscopic plane plasma waves as a superposition of plasmons which are in phase and have the same frequency. The damping of such waves is the net rate at which plasmons disappear from the wave. The condition for the dominance of the resonance is found from the conductivity sum rule.

Transverse

The collective effects on the propagation of transverse photons in the medium can be treated in a completely parallel way. First, we note that the "bare" photon propagator $D_{ij}{}^0$ in Eq. (4.19), is singular for values of k_0 near $\pm c|\mathbf{k}|$. For any diagram in which a factor $\tilde{D}_{ij}{}^0(\mathbf{k},k_0)$ occurs, there are higher order diagrams obtained by inserting any number of polarization bubbles into the photon line as in Fig. 4(a′). We define a transverse proper polarization part $c^{-2}\tilde{Q}_T(\mathbf{k},k_0)\times(\delta_{ij}-k_ik_j/k^2)$. Then the renormalized photon propagator is

$$\tilde{D}_{ij}(\mathbf{k},k^0)=\frac{c^2(\delta_{ij}-k_ik_j/k^2)}{k_0{}^2-k^2c^2+\tilde{Q}_T(\mathbf{k},k_0)}. \tag{4.31}$$

The rules for computing $\tilde{Q}_T(\delta_{ij}-k_ik_j/k^2)$ are the same as for $\tilde{Q}$ except that the current-measuring vertices have the factors of rules (4a) and (5). To obtain $\tilde{Q}_T$ we take the correct transverse projection by averaging over polarizations, i.e., by multiplying by $\frac{1}{2}(\delta_{ij}-k_ik_j/k^2)$ and summing over i and j. The lowest order contribution arising from Fig. 4(c′) is then

$$\tilde{Q}_T{}^0(\mathbf{k},k_0)=\frac{4\pi e^2}{m^2}\int\frac{d^3p}{(2\pi)^3}\frac{1}{2}\left[\mathbf{p}^2-\frac{(\mathbf{p}\cdot\mathbf{k})^2}{k^2}\right]\times\frac{f(\xi_{\mathbf{p}+\mathbf{k}})-f(\xi_{\mathbf{p}})}{k_0-\xi_{\mathbf{p}+\mathbf{k}}+\xi_{\mathbf{p}}}-\Omega_p{}^2. \tag{4.32}$$

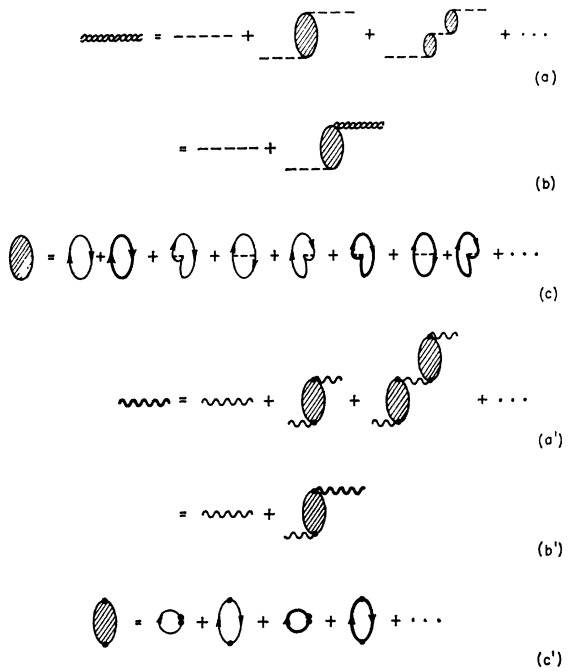

FIG. 4. Polarization corrections to interaction propagators. For the Coulomb interaction: (a) infinite series of corrections; (b) equivalent integral equation; (c) proper longitudinal polarization part. For the transverse photon propagator (a′), (b′), and (c′) are the corresponding transverse relations.

Near the points $\omega=\pm c|\mathbf{k}|$ we again see that the perturbation expansion of $\tilde{D}_{ij}$ in powers of $\tilde{Q}_T$ fails, and we must regard Eq. (4.31) as the correct propagator in the medium. We may also write the expansion for $\tilde{D}_{ij}$ in terms of a transverse dielectric constant

$$\tilde{D}_{ij}(\mathbf{k},k_0)=\tilde{D}_{ij}^{0}(\mathbf{k},k_0)/\tilde{\epsilon}_T(\mathbf{k},k_0), \tag{4.33}$$

where

$$\tilde{\epsilon}_T(\mathbf{k},k_0)=1+\tilde{Q}_T(\mathbf{k},k_0)/(k_0^2-c^2k^2). \tag{4.34}$$

The analytic continuation of $\tilde{\epsilon}_T(\mathbf{k},k_0)$ to continuous $k_0=\omega+i\epsilon$ is $\epsilon_T(\mathbf{k},\omega)$ defined in Eq. (3.2) and the local transverse conductivity is related to the coefficient of the transverse proper polarization part[14]

$$4\pi\omega\sigma_T(\mathbf{k},\omega)=Q_T^{+}(\mathbf{k},\omega). \tag{4.35}$$

This relation and Eqs. (3.7) and (3.11) allow us to compute the properties of transverse electromagnetic waves in a plasma of interacting charged particles. The comments relating the quantized plasmon to the macroscopic plasma wave are immediately generalized to establish the connection between the transverse photons in the medium and the macroscopic transverse waves.[24]

Properties in Simple Pair Approximation

We list here the results, which are all well known, for the energy and damping of longitudinal and transverse waves in the approximation in which only the simple pair bubble diagrams are considered for Q_T and Q.

We are interested in the high-frequency mode which obeys the well-known dispersion formula

$$\Omega^2(\mathbf{k})=\Omega_p^2+k^2\langle v^2\rangle+O(k^4). \tag{4.36}$$

The damping in this case can be calculated from Eq. (4.27). Using Eq. (3.10) we have for the normalization:

$$Z_L^{-1}=1+O(k^2), \tag{4.37}$$

so that the damping is given by

$$\gamma(k)=[1+O(k^2)]4\pi\ \mathrm{Im}\sigma_L(\mathbf{k},\Omega). \tag{4.38}$$

For our later calculations of the collision absorption of transverse waves we need the normalization factor of Eq. (3.11). Using Eqs. (4.32) and (4.35) we find to lowest order in e^2

$$Z_T^{-1}=1+O(k^2). \tag{4.39}$$

Thus, to calculate the lowest order damping of transverse photons, we have

$$\gamma_T(\mathbf{k})=4\pi[1+O(k^2)]\ \mathrm{Im}\sigma_T(\mathbf{k},\omega_T). \tag{4.40}$$

The remainder of this paper is primarily concerned with the calculation of collision contributions to the absorptive process, which we have just seen are either zero or exponentially small in the pair approximation in the regions of interest for transverse and longitudinal electromagnetic waves. In the limit $k^2\ll 1$ we have the inequality $k^2\langle v^2\rangle/\omega^2\ll 1$. Since the absorptive effects are essentially zero in the simple pair approximation, we expect that even if the interactions are weak, the collision effects are the primary contributions. The reactive parts, i.e., the energies (or frequencies) of the waves, were finite in the simple pair approximation so that the collision corrections are relatively small and, therefore, of less interest.

Higher-Order Polarization Parts

Classical and Nonrelativistic Limits

We now turn to the main task of this paper, which is the calculation of higher order proper polarization parts, or what amounts to the same thing [see Eqs. (4.30 and 4.35)], higher order contributions to the local conductivities.

In Figs. 3(b), and 3(c) are displayed the primitive diagrams for the polarization parts to second order in the longitudinal interaction. Interactions via the transverse photons [such as in Fig. 2(c)] are neglected since we consider only the nonrelativistic limit.

It is convenient to distinguish between "classical" diagrams which have a finite contribution in the limit of high temperatures and low densities (or as $\hbar\to 0$) and exchange diagrams which vanish in the limit. It is clear on physical grounds that interactions which involve the exchange of identical particles must vanish

[24] The conditions under which the resonance exhausts the spectrum in the transverse case are given in Appendix A of reference 14.

in the classical limit. It is also clear that all exchange interactions involve interactions with hole lines, either annihilation of a hole by an unrelated particle (exchange of an excited fermion with a fermion in the medium) or the scattering of a hole line into another state (exchange of two fermions in the medium). The only nonexchange interaction involving holes is the creation of a particle-hole pair and the subsequent annihilation of the *same* pair. Thus, we are led to the following rule: *Classical diagrams are those which possess at least one time ordering of the interaction vertices in which there is no more than one hole line per closed loop.* All other diagrams are exchange diagrams and vanish in the classical limit.

A more useful and equivalent rule to determine which primitive diagrams have this property is the *collapsing* rule: In each closed loop of a diagram the particle and the hole lines are collapsed into each other. Those interaction lines which disappear in this process are exchange interactions, and diagrams containing them are exchange diagrams. Thus, diagrams in Fig. 3(c) are exchange diagrams while those in Fig. 3(b) are not.

Applying the collapsing rule, we find that there are no primitive classical diagrams of first order. The complete set of five second-order primitive classical diagrams are shown in Fig. 3(b) for the one-component electron gas. For the two-component system we have the additional 15 diagrams obtained from these by replacing electron closed loops by ion closed loops in all possible combinations. As we have noted (and see in detail) the primitive perturbation expansion does not converge due to the long range of the Coulomb interaction. If we include all polarization effects in the Coulomb lines of the diagrams discussed above, we introduce the effective interaction V. The calculation of these diagrams is our major concern.

Examples of the calculation of higher-order diagrams using the closed diagram rules as discussed above are given in references 5 and 14. In the next two sections we present the details of a simpler and more direct open-diagram calculation method which is entirely equivalent to the methods illustrated in references 5 and 14.

It should be clear how to generalize these arguments to obtain the classical diagrams of higher order in the interaction. A discussion of the size of terms in the classical limit is given in Sec. VI.

V. CALCULATIONS OF DISSIPATIVE PARTS

The dissipative or absorptive properties of the system come directly from the spectral function $A_{ij}(\mathbf{k},\omega)$, which was defined in Eq. (4.12). This function plays a central role in this paper.

As we have seen, the diagrammatic expansion for $\tilde{\Pi}_{ij}$ consists of a series of closed diagrams, each starting from a current measuring vertex and ending in another current measuring vertex. In Fig. 3(a) we show the basic closed diagrams for the decay of radiation to a two-particle state. All the diagrams needed for this calculation are obtained by inserting into these basic diagrams two current- (or charge-) measuring vertices in all topologically distinct ways. The important diagrams for our work are shown in Figs. 3(b) and 3(c). (The remaining diagrams contribute small corrections to the one pair rates, as discussed below.) To get the imaginary part of a diagram one can straightforwardly compute the entire diagram, for example, by the rules in the previous section, perform the analytic continuation, and then take the imaginary part. In recent years, however, there have been developed powerful methods for analyzing the analytic properties of Feynman diagrams and directly obtaining the imaginary parts for the much more complicated problems of relativistic field theories.[25]

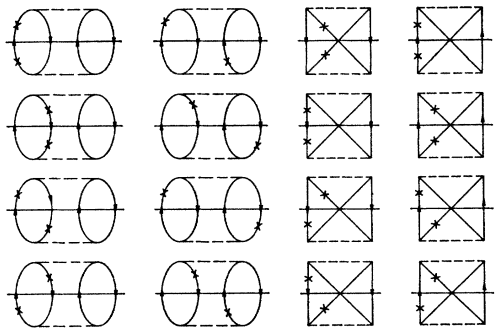

FIG. 5. Cuts of second-order diagrams leading to two-pair states. [These are all the possible two-pair cuts of diagrams 3(b) and (c).]

The spectral function $A_{ij}(\mathbf{k},\omega)$, or equivalently $-\mathrm{Im}\tilde{\Pi}_{ij}{}^{+}(\mathbf{k},\omega)$, is essentially the discontinuity in $\Pi_{ij}{}^{+}(\mathbf{k},\omega)$ across a branch line along the real axis in the ω plane. In pictorial terms this is described in terms of certain cuts across closed diagrams. In Fig. 5 we have shown all the cuts across closed diagrams with a two-pair intermediate state which contribute to the spectral function. All cuts of diagrams in Fig. 6 lead to one-pair intermediate states. One can derive a set of simple rules for obtaining these discontinuities, and thus $\mathrm{Im}\Pi_{ij}{}^{+}$, starting from the closed diagrams.[25] This approach has also been applied to the many-body problem at zero temperature.[9,26] The only difficulty with this procedure is that in higher order there may be

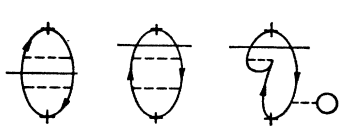

FIG. 6. Second-order diagrams which have cuts only involving one-pair states. [These diagrams are derived from the third and fourth diagrams of Fig. 3(a).]

[25] R. E. Cutkosky, J. Math. Phys. **1**, 429 (1960).

[26] Langer's work (reference 8) emphasized the concept of the quasi-particle which is represented by the completely corrected one-particle propagator. This is useful near $T=0$ where a sharp Fermi surface exists and the one-particle spectral function is nearly a delta function for particles near the surface.

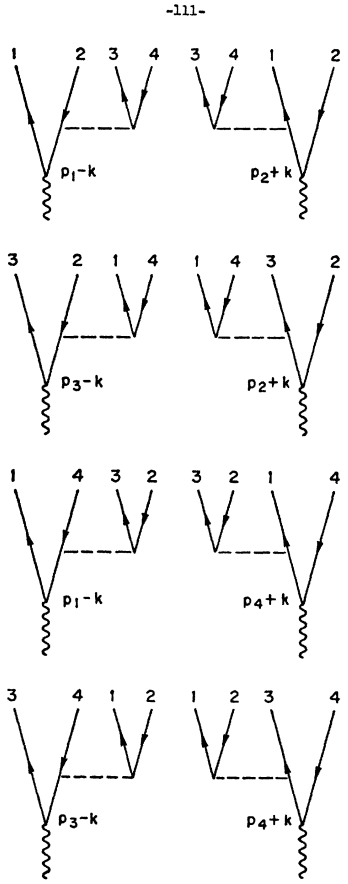

FIG. 7. Complete set of first-order open diagrams for two-pair final state.

a very large number of closed diagrams, each of which can often be cut in several ways to lead to a variety of intermediate states. For instance in Fig. 5 we have sixteen cuts leading to a two-pair final state.

A more direct method of calculating is suggested by the form of Eq. (4.12). Let us rewrite it in the form

$$\begin{aligned} e_i e_j A_{ij}(\mathbf{k},\omega) &= -e_i e_j \,\mathrm{Im}\Pi_{ij}{}^{+}(\mathbf{k},\omega) \\ &= \tfrac{1}{2}\sum_{n,m} \varrho_n \langle n|\hat{e}\cdot\mathbf{J}(0)|m\rangle\langle m|\hat{e}\cdot\mathbf{J}(0)|n\rangle \\ &\quad \times (2\pi)^3\delta^3(\mathbf{k}-\mathbf{P}_m+\mathbf{P}_n) \\ &\quad \times 2\pi[\delta(\omega-E_m+E_n)-\delta(\omega+E_m-E_n)]. \end{aligned} \tag{5.1}$$

The result is analogous to the familiar expression obtained from the requirement that the scattering matrix be unitary,

$$\begin{aligned} -\mathrm{Im}\langle n|R(\omega)|n\rangle &= \tfrac{1}{2}\textstyle\sum_m |\langle m|R(\omega)|n\rangle|^2 \\ &\quad \times (2\pi)^3\delta^3(\mathbf{k}-\mathbf{P}_m+\mathbf{P}_n)2\pi\delta(\omega-E_m+E_n), \end{aligned} \tag{5.1a}$$

and it strongly suggests that the spectral function can be written directly as a rate of an absorption process in terms of amplitudes to the various possible final states, without first considering closed diagrams.[27] The significance of the antisymmetrized energy delta functions is clear: The first term for positive ω is proportional to the probability of absorption where the system is excited from an initial state n to a higher energy state m, while the second term represents the emission probability where the final state m has lower energy than n. Thus, the damping rates or conductivities which we are computing take into account the competition between absorption and emission as they should. If we are to compute the damping of electromagnetic waves in a medium, we must recognize that photons (or plasmons) may be absorbed by the medium or emitted and that we cannot distinguish between photons emitted by the medium and the original photons. Near equilibrium the low-energy states are more heavily occupied than the higher ones, and absorption is greater than emission. If, however, the energy distribution is inverted by some external mechanism such as occurs in a two-stream problem, it may be possible to have a net emission and therefore to produce *growing* waves.

Taking the analogy noted between Eqs. (5.1) and (5.1a) as a point of departure, we propose to calculate the absorptive parts of the propagators directly from open diagrams. We have not proved this procedure in general, and all the calculations reported here have been verified by doing them the usual way, but the analogy is so suggestive that it would be very surprising if the direct method were not correct to all orders.

In general, calculation with open diagrams (as opposed to closed diagrams) is much simpler and there are fewer terms to consider. To use the same example as above, if we are interested in the two-pair final state, we have simply the absolute square of the diagrams in Fig. 7 summed over final states. A computational advantage of this procedure is that cancellations among amplitudes can take place within the absolute value signs. The reader can easily convince himself that squaring the sum of the amplitudes in Fig. 7, that is, connecting them up in all possible ways, gives exactly four times the sum of all the cut closed diagrams in Fig. 5.

The result is hardly surprising. The rate of absorption of radiation to a given final state is the sum of all the processes leading to that final state. For the total absorption rate one averages over initial states and sums over all possible final states. So far, the result appears to be simply the standard quantum-mechanical rule familiar from time-dependent perturbation theory. There is, however, a difference which becomes apparent when one considers a more complicated vertex. If there are internal dummy energy variables, then these are summed over *discrete* indices as in the closed diagram rules in Sec. IV. After the internal sums are carried out, the resulting expression is analytically continued to continuous $\omega \to \omega+i\epsilon$ by the procedure described in Sec. IV. An example of this procedure is given in the next section.

The new rules for the contribution to $4\pi\,\mathrm{Im}\sigma_L$ and

[27] Such a procedure was used in reference 23 to calculate the collision damping of plasmons at $T=0$.

$4\pi\ \mathrm{Im}\sigma_T$ from the decay into a particular final state can be stated in the following simple way[28]:

(1) Write down all topologically distinct, open diagrams leading from the initial state to the final state.

(2) To obtain the amplitude associated with each diagram, write down the internal parts of the open diagram using the rules for closed diagrams in Sec. IV. For each internal line put the appropriate propagator, for each vertex put the appropiate interaction, etc.

(3) Add all amplitudes to the same final state and take the absolute square.

(4) Multiply by $(2\pi)^3$ times a momentum conserving δ function and by 2π times an energy conserving δ function antisymmetrized in the frequency variable, i.e.,

$$(2\pi)^3\delta^3(\mathbf{k}-\mathbf{P}_m+\mathbf{P}_n)\times 2\pi[\delta(\omega-E_m+E_n)-\delta(-\omega-E_m+E_n)].$$

(5) Multiplying by normalizing factors $(1/2\omega)$ for external bosons (i.e., plasmons or photons). For the longitudinal conductivity multiply by an additional factor $(\omega/k)^2$ [see Eq. (4.30)]. For the transverse conductivity multiply by a factor c^2.

(6) Integrate over all final states and average over initial states. We have the usual

$$\int\frac{d^3p}{(2\pi)^3},$$

but, in addition, Fermi particles get a factor $1-f(\xi_p)$ and holes a factor $f(\xi_p)$, where $f(\xi_p)=(1+e^{\beta\xi_p})^{-1}$ and $\xi_p=(\mathbf{p}^2/2m)-\mu$.

(7) When dealing with identical particles, some of the diagrams will be exchange diagrams. The exchange diagrams require a factor (-1) and it is then necessary to divide the rate by a factor $(n)!$ for each type of particle (or hole) where n is the number of particles (or holes) of that type in the final state. This allows us to integrate over all phase space for each particle without counting the same process more than once.

The whole procedure can best be explained by an example. We give the expression for the two-pair collision contribution to the absorptive part of the transverse conductivity of an electron gas, which Eq. (4.40) shows is essentially the damping rate for transverse radiation. We include here the dynamic screening of the interaction. This expression is used for calculations in Sec. VII. From Fig. 7 and the rules given above, we have (with $\hbar=1$)

$$\begin{aligned}4\pi\ \mathrm{Im}\sigma_T(\mathbf{k},\omega)=&\frac{4\pi e^6}{m^2}\int\frac{d^3p_1}{(2\pi)^3}\int\frac{d^3p_2}{(2\pi)^3}\int\frac{d^3p_3}{(2\pi)^3}\int\frac{d^3p_4}{(2\pi)^3}\\
&\times[1-f(\xi_1)]f(\xi_2)[1-f(\xi_3)]f(\xi_4)(2\pi)^3\delta^3(\mathbf{k}-\mathbf{p}_1+\mathbf{p}_2-\mathbf{p}_3+\mathbf{p}_4)\\
&\times 2\pi[\delta(\omega-\xi_1+\xi_2-\xi_3+\xi_4)-\delta(-\omega-\xi_1+\xi_2-\xi_3+\xi_4)]\\
&\times\frac{1}{2\omega}\cdot\frac{1}{4}\Big|V(\mathbf{p}_3-\mathbf{p}_4,\xi_3-\xi_4)\Big[\frac{\hat{e}\cdot\mathbf{p}_1}{\xi_1-\omega-\xi(\mathbf{p}_1-\mathbf{k})}+\frac{\hat{e}\cdot\mathbf{p}_2}{\xi_2+\omega-\xi(\mathbf{p}_2+\mathbf{k})}\Big]\\
&-V(\mathbf{p}_1-\mathbf{p}_4,\xi_1-\xi_4)\Big[\frac{\hat{e}\cdot\mathbf{p}_3}{\xi_3-\omega-\xi(\mathbf{p}_3-\mathbf{k})}+\frac{\hat{e}\cdot\mathbf{p}_2}{\xi_2+\omega-\xi(\mathbf{p}_2+\mathbf{k})}\Big]\\
&-V(\mathbf{p}_3-\mathbf{p}_2,\xi_3-\xi_2)\Big[\frac{\hat{e}\cdot\mathbf{p}_1}{\xi_1-\omega-\xi(\mathbf{p}_1-\mathbf{k})}+\frac{\hat{e}\cdot\mathbf{p}_4}{\xi_4+\omega-\xi(\mathbf{p}_4+\mathbf{k})}\Big]\\
&+V(\mathbf{p}_1-\mathbf{p}_2,\xi_1-\xi_2)\Big[\frac{\hat{e}\cdot\mathbf{p}_3}{\xi_3-\omega-\xi(\mathbf{p}_3-\mathbf{k})}+\frac{\hat{e}\cdot\mathbf{p}_4}{\xi_4+\omega-\xi(\mathbf{p}_4+\mathbf{k})}\Big]\Big|^2. \qquad (5.2)\end{aligned}$$

We have used the notation

$$\xi(\mathbf{p})=(\mathbf{p}^2/2m)-\mu,\quad \xi_a=\xi(\mathbf{p}_a), \qquad (5.3)$$

and $V(\mathbf{p}_a-\mathbf{p}_b,\xi_a-\xi_b)$ is the analytic continuation of the screened interaction defined in Sec. IV. The factor $\frac{1}{4}$ takes account of the extra exchange terms which arise. The analytic continuation procedure prescribes that ω in this equation be understood as $\omega+i\epsilon$.

In the classical limit some simplification is possible. We can separate the amplitudes into those that come from an even or odd number of particle (or hole) exchanges in the basic diagram. The absolute square of one set can be obtained from the other by a change of variables so that we need consider, say, only the even permutations, and then multiply the result by 2. This

[28] We give here the rules for the *local* conductivities which are related to *proper* diagrams. The complete expansion for $\mathrm{Im}\tilde{\Pi}_{ij}$ or, equivalently, the external conductivities, which includes all improper diagrams is found from the relations $\mathrm{Im}\sigma_L^0=\mathrm{Im}\sigma_L|\epsilon_L|^{-2}$, $\mathrm{Im}\sigma_T^0=\mathrm{Im}\sigma_T|\epsilon_T|^{-2}$. In fact, if we apply the rules (2)–(7) to the complete set of diagrams (including improper ones) these relations follow immediately; the extra factors $|\epsilon_L|^{-2}$ and $|\epsilon_T|^{-2}$ arising from the polarization corrections to the incoming lines.

reduces the calculation in the electron gas case to an integral over the absolute square of four amplitudes. However, we shall show in the next section that the order of a diagram in the classical low density limit is not given by the number of interaction lines, because of the dependence of the chemical potential on the effective coupling constant.

VI. CLASSICAL PLASMAS

This section is devoted to a detailed calculation of the conductivity in hot, classical plasmas. The calculating rules of Sec. IV and V are put into a form that is especially convenient in this limit.

Practical Rules and Units

In addition to the external variables $\mathbf{k}$ and ω, the electromagnetic properties of a classical electron gas can depend only on the parameters, e, m, β, and n. In a two-component plasma, such as an electron-ion plasma, there is one additional parameter $\alpha^2=m/M$.

A perturbation expansion for a physical quantity is an expansion in powers of one or more dimensionless parameters. The only dimensionless parameter that can be formed from e, m, β, and n is $e^2n^{1/3}\beta$ which, in fact, does not depend on the mass m. This parameter is essentially the ratio of potential to kinetic energy per particle. Actually, it turns out that the coupling constant which arises naturally is $(e^2n^{1/3}\beta)^{3/2}$ or $\lambda=k_D{}^3/n$, where $k_D=(4\pi e^2n\beta)^{1/2}$ is the Debye wave number. This coupling constant is the ratio of the volume per particle to the cube of the Debye length.

To obtain classical or semiclassical results we must expand in powers of the quantum constant $\hbar$. Consequently, we want to choose units in such a way that $\hbar$ appears explicitly. In any case, at very high temperatures and low densities it is not possible to eliminate $\hbar$ from all results. Since our unit of energy is β^{-1} and the natural unit of frequency is the electron plasma frequency $\Omega_p=(4\pi e^2n/m)^{1/2}$, we immediately have $(\beta\Omega_p)^{-1}$ as the unit of action (and, therefore, of $\hbar$). Furthermore, since the same constant relates momentum and wave number, our choice of k_D as the unit of wave number fixes the unit of momentum to be the thermal momentum $p_T=(m/\beta)^{1/2}$. Of course, $p_T/k_D=(\beta\Omega_p)^{-1}$.

We now rewrite the rules for computing amplitudes from diagrams, entirely in terms of the dimensionless parameters λ, $\hbar$, and α. We then obtain results directly in terms of the physically significant parameters.

In these units the rules for calculating diagrams take the following simple form. We let $\mathbf{p}$ and p_0 denote particle momentum and energy; $\mathbf{k}$ and ω are wave number and frequency of the incoming radiation all measured in our new system of units.

To each element in a diagram corresponds an appropriate factor:

(1a) For each electron line carrying momentum $\mathbf{p}$ and energy put p_0 the electron propagator

$$i/(p_0-\tfrac{1}{2}\mathbf{p}^2+\mu_e).$$

(1b) For each ion line carrying momentum $\mathbf{p}$ and energy p_0 put the ion propagator

$$i/(p_0-\tfrac{1}{2}\alpha^2\mathbf{p}^2+\mu_i).$$

(2) For each Coulomb interaction carrying momentum $\hbar\mathbf{q}$ put $-i\lambda/q^2$.

(3) For each transverse photon line carrying momentum $\hbar\mathbf{k}$ and energy $\hbar\omega$ put the photon propagator

$$\frac{ic^2}{\omega^2-c^2k^2}\left(\delta_{ij}-\frac{k_ik_j}{k^2}\right),$$

where c is the speed of light in units of Ω_p/k_D.

(4a) For each single photon-electron vertex put $-i(\lambda^{1/2}/c)\hat{e}\cdot\frac{1}{2}(\mathbf{p}+\mathbf{p}')$ where $\hat{e}$ is the photon polarization and $\mathbf{p}$ and $\mathbf{p}'$ are the initial and final electron momenta.

(4b) For each single photon-ion vertex put

$$-i\alpha^2(\lambda^{1/2}/c)\hat{e}\cdot\tfrac{1}{2}(\mathbf{p}+\mathbf{p}').$$

(5a) For each double photon-electron vertex put $(\hat{e}\cdot\hat{e}')i\lambda/c^2$.

(5b) For each double photon-ion vertex put

$$(\hat{e}\cdot\hat{e}')i\alpha^2\lambda/c^2.$$

(6) For each closed fermion loop put a factor (-1).

(7) To conserve energy and momentum put delta functions at each vertex

$$-i\hbar^3(2\pi)^3\delta^3(\mathbf{p}'+\mathbf{q}-\mathbf{p})\delta(p_0'+q_0-p_0).$$

(8) Internal momentum and energy variables are summed and integrated over

$$i\sum_{p_0}\int\frac{d^3p}{(2\pi\hbar)^3},$$

with $p_0=i\pi\kappa$, where κ runs over odd integers for fermions and over even integers for bosons.

The open-diagram rules in these units are obvious by comparison with the form given in Sec. V. In the classical limit the distribution functions for holes in the final states become $\exp(-\frac{1}{2}p^2+\mu_e)$ for electrons and $\exp(-\frac{1}{2}\alpha^2p^2+\mu_i)$ for ions. To lowest order we have

$$e^{\mu_e}=\hbar^3(2\pi)^{3/2}\lambda^{-1},$$
$$e^{\mu_i}=\hbar^3(2\pi)^{3/2}\alpha^3\lambda^{-1}.$$

This form is especially convenient for doing classical and semiclassical problems since it is easy to see the order of the diagrams, both in λ and $\hbar$. In doing classical calculations we drop all terms which vanish as $\hbar\to 0$, retaining only those $\hbar$-dependent terms which are necessary to obtain a convergent result. We see that in the case of very high temperatures we are left with a term proportional to $\ln(\hbar)$.

Although these rules allow us to write down a power-series expansion for σ_{ij} in powers of λ, the convergence of this series for $\lambda < 1$ also depends on the value of the external frequency ω. As is seen, in the limit as $k \to 0$ certain energy denominators are proportional to ω with the result that the actual expansion parameter is Γ_c/ω where Γ_c is an effective collision frequency which is proportional to λ and is defined below. For $\omega > \Gamma_c$, which is the case for electromagnetic waves in a plasma, a convergent result is obtained by considering only the lowest order collision diagrams.[5] For $\omega \ll \Gamma_c$, an infinite subseries of diagrams must be summed to obtain a convergent result. This limit is discussed elsewhere. The existence of two limits relative to a collision frequency is well known in the theories of frequency-dependent conductivity.

Classification of Diagrams

The various modes of absorption can be classified according to the number of particles in the final state. Of course, all amplitudes leading to the same final state add coherently. Let us examine some of these modes.

(*i*) *One-Pair Final State*

A transverse photon cannot decay into one pair because energy and momentum cannot be conserved but a longitudinal photon, or plasmon, can decay in this manner. The classical limit of the lowest order process shown in Fig. 8(a) corresponds to the celebrated Landau damping which is the classical limit of the result calculated in Sec. IV. We repeat the classical calculation in this section. The other diagrams shown in Fig. 8 are typical higher order corrections, both in λ and $\hbar$, to the diagram in Fig. 8(a). The diagrams in Figs. 8(e) and 8(f) vanish in the classical limit. Figures 8(b), 8(c), and 8(d) represent vertex corrections to the Landau process. We later show that though Landau damping is the lower order decay mode it is not important for long wavelengths. This is because of its unique exponential dependence on wave number.

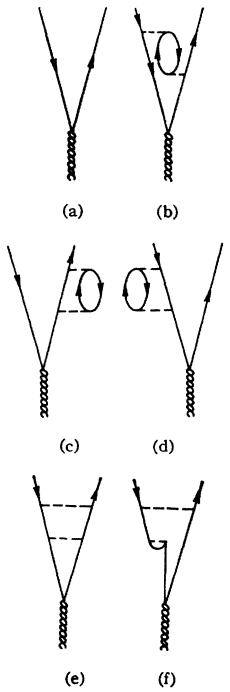

FIG. 8. Open diagrams contributing to one pair or Landau damping process. (a) Lowest order Landau damping process; (b), (c), (d) classical vertex corrections to (a); (e) and (f) quantum vertex corrections to (a).

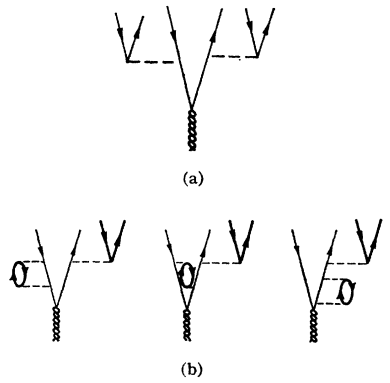

FIG. 9. Higher order diagrams. (a) One contribution to the three electron collision process; (b) corrections to electron-ion collision process, which contain an additional one (electron-hole) pair intermediate state.

If the calculation is carried beyond the lowest order in λ, then it is also necessary to correct the chemical potential which, it should be recalled, is determined separately from the condition on the density of the system. However, we see that because of the limited amount of phase space available for this decay, Landau damping, with its vertex and μ corrections, is not important for $k \ll k_D$.

(*ii*) *Two-Pair Final State*

The lowest order damping process involving collisions, or collision damping, leads to a two-pair final state. It is the chief result of this section that collision damping, though a higher order process, is the dominant damping mode for all but short wavelengths.

Figures 7 and 10 show the lowest order collision processes without screening. All polarization corrections must be summed and they yield the familiar frequency-dependent screened interaction.

The process pictured in Fig. 9(a) is of higher order in λ than the processes of Fig. 7 [in fact, $O(\lambda^2)$], but not of lower order in k^2, so that this and other higher order processes can be neglected when the coupling is weak. However, Fig. 9(b) while one order higher in λ than Fig. 10 also contributes an extra factor ω^{-1}. Only for sufficiently large ω (i.e., $\omega > \Gamma_c$) can Fig. 9(b) be considered a higher order correction. These effects are discussed below where we show that for electromagnetic waves in a plasma $\omega \gg \Gamma_c$ provided $\lambda \ll 1$.

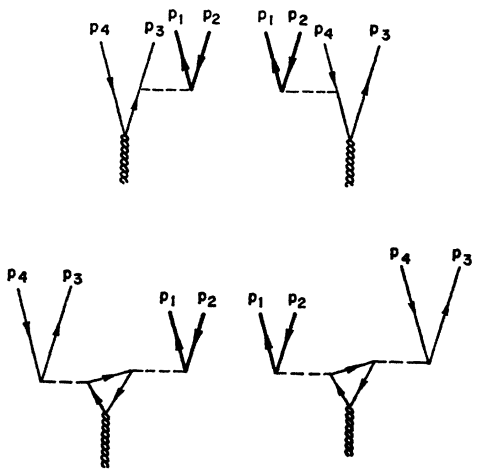

FIG. 10. Open diagrams for decay into a final state of one ion pair plus one electron pair.

Calculations

(i) *Approximations*

It is useful to collect at the outset the various approximations which we make in the following calculation.

(a) First, we are considering the long-wavelength limit ($k \to 0$). In this limit the plasmon and photon are well-defined excitations. Furthermore, we take the limit in such a way that $k/\omega \to 0$ which is consistent with the requirement $\omega > \Gamma_c$.

(b) The weak-coupling approximation requires $\lambda \ll 1$.

(c) We assume that $\hbar \ll 1$, and in order that we may expand the quantum distribution function we also need $\hbar^3/\lambda \ll 1$. In ordinary units we require

$$k_D{}^3 \ll n \ll k_T{}^3, \tag{6.1}$$

where $\hbar k_T = p_T$.

(d) We assume that collisions can be treated by the Born approximation. This means $\beta^{-1} \gg e^4 m/\hbar^2$ or, equivalently, $e^2\beta \ll k_T{}^{-1}$. The first form of the inequality states that the mean kinetic energy must be large compared to a rydberg. In a cooler plasma, the Born approximation is not valid and the situation becomes more complicated. The classical distance of closest approach for a repulsive potential is then roughly $e^2\beta$, the distance at which the potential energy is β^{-1}. Only when $e^2\beta$ becomes much smaller than $k_T{}^{-1}$, the thermal de Broglie wavelength, does the Born approximation apply, for then $e^2\beta \ll \hbar(\beta/m)^{1/2}$, or $(e^2/\hbar\bar{v}) \ll 1$, where $\bar{v} = (m\beta)^{-1/2}$. To go beyond the Born approximation it is necessary to sum all ladder interactions between the colliding particles in the final state which is equivalent to replacing the screened Coulomb interaction by a suitable scattering matrix. This has the effect of replacing $k_T{}^{-1}$ by $e^2\beta$ in the high momentum cutoff of the integrals for the electron gas when $e^2\beta \gg k_T{}^{-1}$. In the electron-ion case no such classical limit exists due to the possibility of forming bound states.

(e) In examining the electron-ion plasma we also neglect terms $O(\alpha)$.

(ii) *Landau Damping*

The lowest order dissipative process is the decay of a plasmon into an electron hole pair (photons do not decay in this order).

We immediately have from the rules [see Fig. 8(a)]

$$4\pi \,\mathrm{Im}\sigma_L = \frac{\omega^2}{k^2}\frac{\lambda}{2\omega}\frac{\hbar^3(2\pi)^{3/2}}{\lambda}\frac{1}{\hbar^6}\int\frac{d^3p_1}{(2\pi)^3}\int\frac{d^3p_2}{(2\pi)^3} \times \hbar^3(2\pi)^3\delta^3(\hbar\mathbf{k}-\mathbf{p}_1+\mathbf{p}_2)2\pi[\delta(\hbar\omega-\tfrac{1}{2}p_1{}^2+\tfrac{1}{2}p_2{}^2) - \delta(-\hbar\omega-\tfrac{1}{2}p_1{}^2+\tfrac{1}{2}p_2{}^2)]\exp(-\tfrac{1}{2}p_2{}^2). \tag{6.2}$$

In the classical limit we obtain the simple result

$$\frac{\gamma}{\Omega_p} = [1+O(k^2)]\left(\frac{\pi}{2}\right)^{1/2} e^{-3/2}\left(\frac{k_D}{k}\right)^3 \exp\left[-\frac{1}{2}\left(\frac{k_D}{k}\right)^2\right]. \tag{6.3}$$

Higher order diagrams such as Figs. 8(b), 8(c), and 8(d) contribute vertex corrections to Landau damping. Without going into the details of such calculations we note that each of these diagrams has the same one-pair final state and therefore the same limited phase space is available. One finds that to order λ the result of including these diagrams is to add to $4\pi \,\mathrm{Im}\sigma_L$ a term of the form

$$\lambda\left(\frac{\omega}{k}\right)^2(2\pi)^{-3}\int d^3p\, C\left(\mathbf{p},\frac{\omega}{k}\right)\exp(-\tfrac{1}{2}p^2)\delta(\omega-\mathbf{p}\cdot\mathbf{k}), \tag{6.4}$$

where $C(\mathbf{p},\omega/k)$ is a decreasing function of $\mathbf{p}$ and ω/k. The function C is obtained as the result of summing and integrating over the internal variables of these diagrams. We are, therefore, assured that the value of this integral differs from the right-hand side of Eq. (6.3) by a factor $\Lambda'(\omega/k)$, which is a decreasing function of ω/k. In addition, corrections to μ must be included to order λ. Writing $e^{\beta\mu} = e^{\beta\mu_0}(1+\beta\delta\mu)$ we find that the one-pair rate corrected to order λ is of the form

$$[1+\Lambda(\omega/k)](\pi/2)^{1/2}(\omega^2/k^3)\exp(-\tfrac{1}{2}\omega^2/k^2), \tag{6.5}$$

where

$$\Lambda(\omega/k) = \Lambda'(\omega/k)+\beta\delta\mu \tag{6.6}$$

is proportional to λ and, therefore, small compared to 1 in the weak coupling limit. From here on we neglect this small term.

Note that the corresponding contribution to $4\pi \,\mathrm{Im}\sigma_L$ from the decay into one ion-hole pair is

$$\left(\frac{\pi}{2}\right)^{1/2}\frac{\omega}{k^2}\frac{\omega}{\alpha k}\exp\left(-\frac{1}{2}\frac{\omega^2}{\alpha^2k^2}\right). \tag{6.7}$$

(iii) Collision Damping

We discuss separately the electron-ion plasma and the electron gas because the situations are somewhat different. We present, in detail, the calculation for the absorption of plasmons in an electron-ion plasma and state the results for other cases of interest. We begin with a discussion of the form of the screened interaction in the classical limit. The details of the screening effects in various frequency limits are treated at the end of the section.

As we pointed out in Sec. IV, after summing all polarization effects the Coulomb interaction is replaced by an energy-dependent interaction $V(\mathbf{p},p_0)$, which in our new units can be written as

$$V(\mathbf{p},p_0)=\frac{\lambda\hbar^2}{p^2+\hbar^2Q(\mathbf{p},p_0)}=\frac{\lambda}{q^2+Q(\mathbf{q},q_0)}, \tag{6.8}$$

where $\mathbf{p}=\hbar\mathbf{q}$, and $p_0=\hbar q_0$.

To obtain results exact to order λ in the two-pair process it is clear from our practical rules that we need include only the lowest order polarization process (of order 1) in Q. Higher order polarization corrections lead to contributions of order λ^2 and higher. In an electron gas Q^0 is the single electron-hole bubble [Fig. 4(c)]. At zero-frequency transfer Q^0, in ordinary units, is just k_D^2. This is the familiar Debye screening factor.

In an electron-ion plasma Q^0 is the sum of an electron bubble and an ion bubble. Let us compute $Q^0(\mathbf{p},p_0,\alpha)$; we can then obtain the electron bubble by putting $\alpha=1$. From our rules we have

$$\mathrm{Im}Q^0(\mathbf{p},p_0,\alpha)=\left(\frac{\pi}{2}\right)^{1/2}\frac{p_0}{\alpha p}\exp\left[-\frac{1}{2}\left(\frac{p_0}{\alpha p}\right)^2\right]. \tag{6.9}$$

To get Q^0 we use the dispersion relation

$$Q^0(\mathbf{p},p_0,\alpha)=\int\frac{du}{\pi}\frac{1}{p_0-u}\,\mathrm{Im}Q^0(\mathbf{p},u,\alpha). \tag{6.10}$$

Explicitly, we have

$$Q^0(\mathbf{p},p_0,\alpha)=(2\pi)^{-1/2}\int du\frac{u}{u-p_0/\alpha p}\exp(-\tfrac{1}{2}u^2). \tag{6.11}$$

We now see that Q^0 is only a function of $p_0/\alpha p$. Note that in the scattering of a light particle from a heavy particle p_0 is small and the result can be independent of α.

We give here a form for $Q^0(z)$ which is useful for numerical calculations

$$\mathrm{Re}Q^0(z)=1-z\exp(-\tfrac{1}{2}z^2)\int_0^z dt\exp(\tfrac{1}{2}t^2) \tag{6.12}$$

$$\mathrm{Im}Q^0(z)=(\pi/2)^{1/2}z\exp(-\tfrac{1}{2}z^2). \tag{6.13}$$

Electron-Ion Plasma

The dominant absorption mode for an electron-ion plasma is shown in Fig. 10. The heavy lines represent ions. Processes which involve absorption of radiation by ions vanish as $\alpha\to 0$. Absorption by an electron with subsequent scattering by another electron is of higher order in k^2 and can be ignored here though it is the leading decay process in an electron gas with a smeared out ion background.

From Fig. 10 we can immediately write down the decay rate for plasmons. [We let $\xi(\mathbf{p})=\frac{1}{2}\mathbf{p}^2-\mu_e$ for electrons and $\frac{1}{2}\alpha^2\mathbf{p}^2-\mu_i$ for ions, and also $\xi(\mathbf{p}_a)=\xi_a$.]

$$\begin{aligned}4\pi\,\mathrm{Im}\sigma_L=&\frac{\lambda}{2\omega}\frac{(2\pi)^3}{\hbar^6}\frac{1}{\lambda^2}\alpha^3\frac{1}{\hbar^{12}}\int\frac{d^3p_1}{(2\pi)^3}\int\frac{d^3p_2}{(2\pi)^3}\int\frac{d^3p_3}{(2\pi)^3}\int\frac{d^3p_4}{(2\pi)^3}\\
&\times\exp(-\tfrac{1}{2}\alpha^2p_2^2)\exp(-\tfrac{1}{2}p_4^2)\hbar^3(2\pi)^3\delta^3(\hbar\mathbf{k}-\mathbf{p}_1+\mathbf{p}_2-\mathbf{p}_3+\mathbf{p}_4)\\
&\times 2\pi[\delta(\hbar\omega-\xi_1+\xi_2-\xi_3+\xi_4)-\delta(-\hbar\omega-\xi_1+\xi_2-\xi_3+\xi_4)]\,|V(\mathbf{p}_1-\mathbf{p}_2,\,\xi_1-\xi_2)|^2\\
&\times\left|\frac{\hat{k}\cdot\mathbf{p}_4}{\hbar\omega-\xi(\mathbf{p}_4+\hbar\mathbf{k})+\xi_4}-\frac{\hat{k}\cdot\mathbf{p}_3}{\hbar\omega-\xi_3+\xi(\mathbf{p}_3-\hbar\mathbf{k})}+V(\mathbf{p}_3-\mathbf{p}_4,\,\xi_3-\xi_4)T(\omega)\right|^2,\end{aligned} \tag{6.14}$$

where the last term in the absolute value sign arises from the closed loops in the two final diagrams of Fig. 10, and where

$$\begin{aligned}T(k_0)=\int\frac{d^3t}{(2\pi)^3}\hat{k}\cdot\mathbf{t}\frac{1}{i}\sum_{t_0}\Bigg\{&\frac{1}{t_0-\hbar k_0-\xi(\mathbf{t}-\hbar\mathbf{k})}\frac{1}{t_0-\xi_t}\frac{1}{t_0-(p_3-p_4)_0-\xi(\mathbf{t}-\mathbf{p}_3+\mathbf{p}_4)}\\
&+\frac{1}{t_0-\hbar k_0-\xi(\mathbf{t}-\hbar\mathbf{k})}\frac{1}{t_0-\xi_t}\frac{1}{t_0-(p_1-p_2)_0-\xi(\mathbf{t}-\mathbf{p}_1+\mathbf{p}_2)}\Bigg\}.\end{aligned} \tag{6.15}$$

The sum over t_0 is readily performed by the method of contour integration (remembering that at this point all quantities with zero subscript take on discrete values). It is convenient at this point to take the long-wavelength

limit ($k/\omega \to 0$) and to perform the change of variables

$$\mathbf{p}_1-\mathbf{p}_2=\mathbf{P}_1, \quad \mathbf{p}_1+\mathbf{p}_2=\mathbf{P}_2, \quad \mathbf{p}_3-\mathbf{p}_4=\mathbf{P}_3, \quad \mathbf{p}_3+\mathbf{p}_4=\mathbf{P}_4. \tag{6.16}$$

We then find, after continuing to continuous values of the various variables (in particular, $k_0 \to \omega+i\epsilon$), that

$$T(\omega)=\frac{\hat{k}\cdot\mathbf{P}_3}{\omega}S(\omega), \tag{6.17}$$

where

$$S(\omega)=\int\frac{d^3t}{(2\pi)^3}\frac{\mathbf{t}\cdot\mathbf{P}_3}{P_3^2}\Big\{[f(\xi_t)-f(\xi(\mathbf{t}-\mathbf{P}_3))]\Big[\frac{1}{\xi_t-\xi(\mathbf{t}-\mathbf{P}_3)+\hbar\omega-\frac{1}{2}\mathbf{P}_3\cdot\mathbf{P}_4}-\frac{1}{\xi_t-\xi(\mathbf{t}-\mathbf{P}_3)-\frac{1}{2}\mathbf{P}_3\cdot\mathbf{P}_4}\Big]$$
$$+[f(\xi_t)-f(\xi(\mathbf{t}+\mathbf{P}_3))]\Big[\frac{1}{\xi_t-\xi(\mathbf{t}+\mathbf{P}_3)+\hbar\omega-\frac{1}{2}\alpha^2\mathbf{P}_1\cdot\mathbf{P}_2}-\frac{1}{\xi_t-\xi(\mathbf{t}+\mathbf{P}_3)-\frac{1}{2}\alpha^2\mathbf{P}_1\cdot\mathbf{P}_2}\Big]\Big\}. \tag{6.18}$$

Using the energy δ function and dropping terms $O(\alpha^2)$ we get

$$S(\omega)=1-Q^0(\hbar\omega/P_3). \tag{6.19}$$

We can now rewrite Eq. (6.14) discarding nonessential terms proportional to $\hbar$:

$$4\pi\,\mathrm{Im}\sigma_L=\frac{\lambda\alpha^3}{128(2\pi)^5}\int d^3P_1\int d^3P_2\int d^3P_3\int d^3P_4\delta^3(\mathbf{P}_1+\mathbf{P}_3)\int du\,\delta(u-\tfrac{1}{2}\mathbf{P}_3\cdot\mathbf{P}_4)\int dv\,\delta(v-\tfrac{1}{2}\mathbf{P}_1\cdot\mathbf{P}_2)\delta(\hbar\omega-u-\alpha^2v)$$
$$\times\exp[-\tfrac{1}{8}(\alpha^2P_1^2+\alpha^2P_2^2+P_3^2+P_4^2)]\Big(\frac{\hat{k}\cdot\mathbf{P}_3}{\omega}\Big)^2|V(\mathbf{P}_1,\alpha^2v)|^2|1+V(\mathbf{P}_3,u)[1-Q^0(u/P_3)]|^2. \tag{6.20}$$

The P_1 integration is trivial. One can also average over the directions of $\hat{k}$. It is now simple to do the P_2 and P_4 integrations and the angular P_3 integrations. (We now let $P_3=P$.) We obtain the result

$$4\pi\,\mathrm{Im}\sigma_L=\frac{\lambda}{12\pi^2\omega^2}\int dPP^3\int du\frac{\alpha}{P}\int dv\,\delta(\hbar\omega-u-\alpha^2v)\exp\Big(-\frac{1}{8}P^2\Big)\exp\Big(-\frac{1}{2}\frac{u^2}{P^2}\Big)\exp\Big(-\frac{1}{2}\frac{\alpha^2v^2}{P^2}\Big)$$
$$\times\frac{1}{|P^2+\hbar^2Q^0(\alpha^2v/P)+\hbar^2Q^0(\alpha v/P)|^2}\frac{(P^2+1)^2}{|P^2+\hbar^2Q^0(\hbar\omega/P)|^2}. \tag{6.21}$$

The u integral is trivial. If we let $P=\hbar q$ and $\alpha v/P=z$ we have

$$4\pi\,\mathrm{Im}\sigma_L=\frac{\lambda}{6\sqrt{2}\pi^{3/2}\omega^2}\int dqq^3\exp\Big(-\frac{1}{8}\hbar^2q^2\Big)\exp\Big(-\frac{1}{2}\frac{\omega^2}{q^2}\Big)\frac{(q^2+1)^2}{|q^2+Q^0(\omega/q)|^2}\frac{1}{\sqrt{2}\pi}\int dz\exp\Big(-\frac{1}{2}z^2\Big)\frac{1}{|q^2+1+Q^0(z)|^2}. \tag{6.22}$$

The z integral can be done analytically,[6] (this was pointed out to us by A. Ron) to yield

$$4\pi\,\mathrm{Im}\sigma_L=\frac{\lambda}{6\sqrt{2}\pi^{3/2}\omega^2}K_a,$$

where

$$K_a=\int dqq^3\exp\Big(-\frac{1}{8}\hbar^2q^2\Big)\exp\Big(-\frac{1}{2}\frac{\omega^2}{q^2}\Big)\frac{q^2+1}{q^2+2}\frac{1}{|q^2+Q^0(\omega/q)|^2}. \tag{6.23}$$

At very high frequencies the screening is unimportant and

$$K_a=\ln(4e^{-C}/\hbar\omega) \quad (\omega\gg1), \tag{6.24}$$

where C is Euler's constant, $C\approx0.58$. At frequencies low compared with the plasma frequency (but still large compared with the collision frequency) we have $K_a\approx\ln(1.06/\hbar)$.

The transverse conductivity is calculated in exactly the same way except that at the start it is necessary to average over the transverse polarization,

$$e_ie_j\to\tfrac{1}{2}(\delta_{ij}-k_ik_j/k^2).$$

The expression simplifies considerably if we then average over the directions of $\hat{k}$.

The result is

$$\mathrm{Im}\sigma_T = \mathrm{Im}\sigma_L. \tag{6.25}$$

The conductivity is related to the width for decay γ of the radiation by Eqs. (4.38) and (4.40). The relation of Eq. (6.25) states that in the limit of long wavelengths an isotropic system responds in the same way to transverse or longitudinal excitations.

We can now express the result of these calculations in the simple form (in ordinary units):

$$4\pi\,\mathrm{Im}\sigma_{ij}(k,\omega) = \frac{\Omega_p}{6\sqrt{2}\pi^{3/2}}\frac{k_D{}^3}{n}\frac{\Omega_p{}^2}{\omega^2}\ln\left[\frac{C_a(\omega)}{\beta\hbar\omega}\right]\delta_{ij}. \tag{6.26}$$

We obtain the contributions to the decay widths due to collision damping by use of Eqs. (4.38) and (4.40). The result for the damping of longitudinal oscillations in an electron-ion plasma, for example, is

$$\gamma_L = \frac{\Omega_p}{6\sqrt{2}\pi^{3/2}}\frac{k_D{}^3}{n}\ln\left[\frac{C_a(\Omega_p)}{\beta\hbar\Omega_p}\right]. \tag{6.27}$$

This is to be compared with the contribution from Landau damping given in Eq. (6.3). It is clear that for long wavelengths the contribution from Eq. (6.27) is far more important.

In Fig. 11 we plot for various values of $\lambda = k_D{}^3/n$ and $\sigma = \beta\hbar\Omega p$ those values of k/k_D for which Landau damping and collision damping are equal. We somewhat arbitrarily pick $k/k_D = 0.3$ as the maximum value of k for which plasma oscillations are well defined, for when k is greater than this value, $\gamma_{\mathrm{Landau}}/\Omega_p > 0.1$, and the plasma wave decays in a few oscillations. From this figure it can be seen that the region to the right of the curves, where collision damping dominates covers a significantly larger range of temperatures and densities than the region to the left of the curves where Landau damping dominates. In Fig. 12 we plot curves of constant σ and λ as functions of T and n^{-1}, which allows us to relate the regions of Fig. 11 to values of temperature and density.

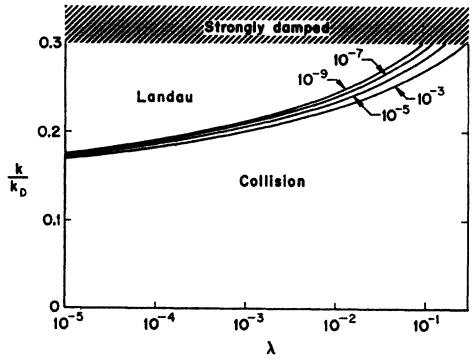

FIG. 11. Values of k/k_D for which Landau damping, Eq. (6.3), and collision damping, Eq. (6.27a), of electron plasma oscillations are equal, plotted as a function of $\lambda = k_D{}^3/n$ for various values of $\sigma = \beta\hbar\Omega_p$. In the strongly damped region, Landau damping alone is greater than $0.3\Omega_p$. In the Landau region Landau damping is larger than collision damping. In the collision region the reverse is true.

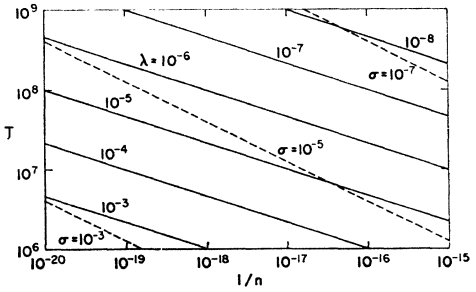

FIG. 12. Curves of constant $\lambda = k_D{}^3/n$ (solid lines) and $\sigma = \beta\hbar\Omega_p$ (dashed lines) as functions of T and n^{-1}.

For multiply charged ions ($Z > 1$) the results in Eqs. (6.26) and (6.27) are changed in two ways: There is an over-all factor of Z and the argument of the logarithms become functions of Z. The argument of the logarithm is changed because the screened interaction denominator in Eq. (6.20) is changed to $|q^2+1+ZQ^0(z)|^2$.

In a previous version of this paper[14] we overlooked the fact (which follows directly from the rules of the original paper) that the lower diagrams of Fig. 10 were of the same order as the upper diagrams in the classical low-density limit. With this correction we are in agreement with the work of Dawson, Oberman, and Ron[6] and Perel and Eliashberg.[5]

ω and k Dependence of Higher Order Diagrams

We have considered all diagrams of order λ in our present calculation. The remaining diagrams are all higher order in λ and $\hbar$. It is still necessary to show that the k^2 and ω dependence of these higher order diagrams does not affect the convergence of the series in the limit $k \to 0$ for the frequencies of electromagnetic waves in plasmas.

The isotropy of the system implies that the conductivities and damping rates are functions of k^2. In calculations of higher order diagrams the expansion of energy denominators in powers of k/ω is again carried out. It then becomes clear that there is no dependence on k^{-2} since no inverse powers of k^2 appear in the formulas for σ_{ij}.

Thus, it appears that the rates or conductivities behave as $\sim$constant$+O(k^2)$ in higher order terms. In the electron-ion case this would lead to a λ^2 correction to the constant term we have already calculated. In the electron gas, since current and momentum are proportional, one expects that electron-electron interactions which conserve momentum do not effect the conductivity in the limit of long wavelengths. It would then appear that in higher orders the increased symmetry of the amplitude leads to additional cancellations as in the second-order calculation above. This implies

that the rates are proportional to k^2 in higher order contributions to the electron gas conductivity.

Likewise, the ω dependence of higher order diagrams causes no difficulty at the frequencies of electromagnetic waves in plasmas. Using the well-known conductivity formula,

$$4\pi \operatorname{Im}\sigma_{ij}=(\Omega_p^2/\omega^2)\Gamma_c(\omega)\delta_{ij}, \tag{6.28}$$

we can identify the collision frequency Γ_c in the electron-ion case as

$$\Gamma_c(\omega)=\frac{\Omega_p}{6\sqrt{2}\pi^{3/2}}\frac{k_D^3}{n}\ln\left[\frac{C_a(\omega)}{\beta\hbar\omega}\right]. \tag{6.29}$$

For values of $\omega<\Gamma_c$, higher order diagrams such as those in Fig. 9(b) become important. These diagrams are characterized by having successively greater numbers of one pair intermediate states each of which contributes a factor $\sim\Gamma_c/\omega$ to the amplitude. If we are interested in the static ($\omega=0$) conductivity this subseries of diagrams must be summed and would be expected to yield $4\pi \operatorname{Im}\sigma_{ij}(0,0)\sim\delta_{ij}[\Omega_p^2/\Gamma_c(0)]$. Details of the calculation in this limit are reserved for another paper. However, for the frequencies of electromagnetic waves in plasmas, $\omega\geq\Omega_p$ the requirement $\Gamma_c/\omega\ll 1$ reduces to $1\gg(k_D^3/6\sqrt{2}\pi^{3/2}n)\ln[C_a(\omega)/\beta\hbar\omega]$. This inequality is satisfied since we are assuming values of n and β such that the inequality (6.1) holds. A similar argument can be made in the electron gas case.

The fact that the two lower diagrams of Fig. 10 contribute to order λ is due to the fact that in the low density limit each closed loop contributes a factor $\exp(\beta\mu)\propto\lambda^{-1}$, which cancels the λ arising from the extra interaction. In the high-density electron gas, which we discuss in the next section, the coupling enters only through the interaction line, and these diagrams are of higher order.

VII. HIGH DENSITY ELECTRON GAS

Preliminary Remarks

In this section we discuss briefly the application of the foregoing techniques to the high-density electron gas. This system is intrinsically quantum mechanical, and the effects of exchange are important. We consider the limit of zero temperature, which merely restricts the usefulness of our results to temperatures for which β^{-1} is small compared with the Fermi energy, $\epsilon_F=p_F^2/2m$, where p_F is the Fermi momentum.

The natural system of units in this case is the one which expresses momenta in terms of the Fermi momentum

$$p_F=\hbar/\alpha r_0,\quad n^{-1}=4\pi r_0^3/3,\quad \alpha=[2/9\pi]^{1/3},$$

and energies in terms of the Fermi energy, ϵ_F. The expansion parameter λ is again a dimensionless ratio of the potential to the kinetic energy:

$$\frac{\text{P.E.}}{\text{2K.E.}}\propto\frac{e^2/r_0}{\hbar^2/m\alpha^2r_0^2}\propto r_s,$$

where $r_s=r_0/a_0$ and a_0 is the Bohr radius, $a_0=\hbar^2/me^2$. In terms of r_s the Fermi energy takes the form $\epsilon_F=(\alpha r_s)^{-2}$ in rydbergs.

Propagator techniques have been used extensively to study the behavior of the quantum electron gas,[21–23] especially its equilibrium properties. The solutions obtained as modified perturbation expansions in powers of r_s are valid only for small r_s, say, $r_s<1$, which implies that they are not valid for a quantitative description of the electron gas in a metal, for which $r_s>2$.

Classification of Diagrams

Diagrams for the construction of $\tilde{\Pi}_{ij}$ still can be classified in terms of the number of pairs in the final state. At zero temperature the particle-hole concept is well known, and the distribution functions become step functions,

$$f(\xi_p)\rightarrow\eta(-\xi_p)=\eta(\mu-p^2/2m),$$

which restrict particle momenta to values greater than p_F and hole momenta to values less than p_F. The general problem (which does not arise in the present calculation) of calculating corrections to the chemical potential μ is simplified in this limit, as has been shown by Luttinger and Ward.[18] The correct prescription is to use μ_0, the chemical potential of the noninteracting system, and to omit certain anomalous self-energy corrections to the Fermion lines.

The lowest order contribution to $\tilde{\Pi}_{ij}$ comes from a simple pair loop. In the case of transverse photons there is again no absorption in this order because momentum and energy cannot be conserved. For longitudinal plasmons, the absorption is a function of the momentum q. To decay into a pair the plasmon energy $\Omega_p(q)$ must be less than the maximum pair energy of the same momentum, $p_Fq/m+q^2/2m$. The critical momentum for decay, q_c, is determined from the relation

$$\Omega_p(q_c)=(p_Fq_c/m)+(q_c^2/2m). \tag{7.1}$$

For $q<q_c$, energy cannot be conserved for plasmon decay into a pair and, therefore, the plasmon can be studied as a unique stable excitation of the system in the pair, or random phase, approximation. For $q>q_c$, on the other hand, the pair decay process is so strong that the plasmons are entirely lost in the continuum of pair states. The details of this argument are given by Ferrell[29] and DuBois.[3] Vertex corrections to the single-pair final-state diagrams do not change this result.

As in the classical case, the important absorptive contributions come from the two-pair final states, properly corrected for collective effects. The diagrams

[29] R. A. Ferrell, Phys. Rev. **107**, 450 (1957).

are those in Fig. 7, including the exchange diagrams. The contributions to plasmon decay in this order and including exchange have been calculated previously by DuBois[3] using open diagram methods.

The calculation of the contributions to photon decay from the two-pair final states is similar to the calculation of plasmon damping. The calculation naturally divides itself into two parts, differentiated by the nature of the final pairs, namely, the two-free-pair final state and the pair-plus-plasmon (or bound-pair) final state. The plasmon-pair final-state contribution deserves some attention since it has recently been proposed[7] that an experimental measurement of the photoabsorption cross section of a metal could yield some information on the collective modes.

To evaluate[30] $\mathrm{Im}\sigma_T$, we start from the diagrams of Fig. 7 and obtain the analytic expression which is given in Eq. (5.2). However, to calculate decay into a pair plus plasmon we need retain in the square of the total amplitude in Eq. (5.2) only the sum of the squares of the bracketed terms because the remaining cross terms contribute only to the two-free-pair decay process. The symmetry of the integral may now be used to simplify the expression. With $\hbar=1$, we have

$$4\pi\,\mathrm{Im}\sigma_T(\mathbf{k},\omega)=\frac{4\pi e^2}{m^2}\int\frac{d^3p_1}{(2\pi)^3}\int\frac{d^3p_2}{(2\pi)^3}\int\frac{d^3p_3}{(2\pi)^3}\int\frac{d^3p_4}{(2\pi)^3}(2\pi)^3\delta^3(\mathbf{k}-\mathbf{p}_1+\mathbf{p}_2-\mathbf{p}_3+\mathbf{p}_4)$$
$$\times 2\pi[\delta(\omega-\xi_1+\xi_2-\xi_3+\xi_4)-\delta(-\omega-\xi_1+\xi_2-\xi_3+\xi_4)][1-f(\xi_1)]f(\xi_2)[1-f(\xi_3)]f(\xi_4)$$
$$\times\frac{1}{2\omega}\left|\frac{4\pi e^2}{(\mathbf{p}_3-\mathbf{p}_4)^2+Q^0(\mathbf{p}_3-\mathbf{p}_4,\,\xi_3-\xi_4)}\right|^2\left[\frac{\hat{e}\cdot\mathbf{p}_1}{\xi_1-\omega-\xi(\mathbf{p}_1-\mathbf{k})}+\frac{\hat{e}\cdot\mathbf{p}_2}{\xi_2+\omega-\xi(\mathbf{p}_2+\mathbf{k})}\right]^2. \quad (7.2)$$

In the dipole approximation ($k\to 0$) the propagators in Eq. (7.2) reduce to $-(1/\omega)$ and $(1/\omega)$, respectively, simplifying the second factor to $(\mathbf{q}\cdot\hat{e})^2/\omega^2$, where $\mathbf{q}=\mathbf{p}_2-\mathbf{p}_1$. With a change of variables to $\mathbf{q}=\mathbf{p}_2-\mathbf{p}_1$, $\mathbf{p}=\frac{1}{2}(\mathbf{p}_1+\mathbf{p}_2)$, $\mathbf{r}=\frac{1}{2}(\mathbf{p}_3+\mathbf{p}_4)$, $\mathbf{s}=\mathbf{p}_3-\mathbf{p}_4$, and the trivial integration over $\mathbf{s}$ we have

$$4\pi\,\mathrm{Im}\sigma_T(\mathbf{k},\omega)=\left[\frac{4e^6}{m^2\omega^3(2\pi)^5}\right]\int d^3q\int d^3p\int d^3r\left[\delta\left(\omega+\frac{\mathbf{p}\cdot\mathbf{q}}{m}-\frac{\mathbf{q}\cdot\mathbf{r}}{m}\right)-\delta\left(-\omega+\frac{\mathbf{p}\cdot\mathbf{q}}{m}-\frac{\mathbf{q}\cdot\mathbf{r}}{m}\right)\right]$$
$$\times[1-f(\xi_{\mathbf{p}-\frac{1}{2}\mathbf{q}})]f(\xi_{\mathbf{p}+\frac{1}{2}\mathbf{q}})[1-f(\xi_{\mathbf{r}+\frac{1}{2}\mathbf{q}})]f(\xi_{\mathbf{r}-\frac{1}{2}\mathbf{q}})\,|q^2+Q^0(q,\mathbf{q}\cdot\mathbf{r}/m)|^{-2}(\hat{e}\cdot\mathbf{q})^2. \quad (7.3)$$

The symmetries of the integral and the properties of the distribution functions can be used to rewrite this integral in the form

$$4\pi\,\mathrm{Im}\sigma_T(\mathbf{k},\omega)=-\left[\frac{4e^6}{m^2\omega^3(2\pi)^5}\right]\int d^3q\int d^3p\,(\hat{e}\cdot\mathbf{q})^2\int du\,|q^2+Q^0(q,u)|^{-2}f(\xi_{\mathbf{p}+\frac{1}{2}\mathbf{q}})[1-f(\xi_{\mathbf{p}-\frac{1}{2}\mathbf{q}})]$$
$$\times g(u)[\delta(\omega+u+\mathbf{p}\cdot\mathbf{q}/m)-\delta(\omega-u-\mathbf{p}\cdot\mathbf{q}/m)]\int d^3r\,[1-f(\xi_{\mathbf{r}+\frac{1}{2}\mathbf{q}})]f(\xi_{\mathbf{r}-\frac{1}{2}\mathbf{q}})\left[\delta\left(u-\frac{\mathbf{q}\cdot\mathbf{r}}{m}\right)-\delta\left(u+\frac{\mathbf{q}\cdot\mathbf{r}}{m}\right)\right], \quad (7.4)$$

where $g(u)=[1-e^{\beta u}]^{-1}$ is the boson distribution function. The integral over r in Eq. (7.4) can readily be shown to reduce to $(2\pi/e^2)\,\mathrm{Im}Q^0(q,u)$ and $\mathrm{Im}\sigma_T$ is then given by

$$4\pi\,\mathrm{Im}\sigma_T(\mathbf{k},\omega)=\left[\frac{4\pi e^2}{m^2\omega^3(2\pi)^6}\right]\int d^3p\int d^3q\,(\hat{e}\cdot\mathbf{q})^2 f(\xi_{\mathbf{p}+\frac{1}{2}\mathbf{q}})[1-f(\xi_{\mathbf{p}-\frac{1}{2}\mathbf{q}})]$$
$$\times\int du\,g(u)\left[\delta\left(\omega+\frac{\mathbf{p}\cdot\mathbf{q}}{m}+u\right)-\delta\left(\omega-\frac{\mathbf{p}\cdot\mathbf{q}}{m}-u\right)\right]\mathrm{Im}V(\mathbf{q},u), \quad (7.5)$$

where we have used the definition

$$V(\mathbf{q},u)=\frac{4\pi e^2}{q^2+\mathrm{Re}Q^0(\mathbf{q},u)+i\,\mathrm{Im}Q^0(\mathbf{q},u)}, \quad (7.6)$$

and the result

$$4\pi e^2\,\mathrm{Im}V(\mathbf{q},u)=-\frac{(4\pi e^2)^2\,\mathrm{Im}Q^0(\mathbf{q},u)}{[q^2+\mathrm{Re}Q^0(\mathbf{q},u)]^2+[\mathrm{Im}Q^0(\mathbf{q},u)]^2}$$
$$=-\mathrm{Im}Q^0(\mathbf{q},u)\,|V(\mathbf{q},u)|^2. \quad (7.7)$$

We identify the plasmon as the δ-function part of $\mathrm{Im}V(\mathbf{q},u)$ in Eq. (7.5) and we remark that caution must be exercised in identifying this piece for, as discussed above, $\mathrm{Im}Q^0(\mathbf{q},u)=0$ only if $q<q_c$, and only for small momenta is there a plasmon delta-function contribution to $\mathrm{Im}V(\mathbf{q},u)$. We, therefore, limit the q integral in Eq. (7.5) to values less than the critical mo-

[30] It should be clear that at $T=0$ $\gamma_T=4\pi\,\mathrm{Im}\sigma_T(\mathbf{k},\omega)$, where $\omega=kc$, is just the absorption rate of external photons by the medium.

mentum, q_c. The part of σ_T contributed by momenta greater than the critical momentum should be grouped with the remaining two-free-pair terms, which we have dropped, for a calculation of the free pair contribution to the absorption of photons.

In the region $q<q_c$ the plasmon contribution to $\mathrm{Im}V(\mathbf{q},u)$ is

$$\mathrm{Im}V(\mathbf{q},u)_{\mathrm{plasmon}}=(4\pi e^2/q^2)[-\pi\Omega_p(\mathbf{q})/2] \times\{\delta[u-\Omega_p(\mathbf{q})]-\delta[u+\Omega_p(\mathbf{q})]\}. \quad (7.8)$$

At zero temperature the boson distribution function in Eq. (7.4) restricts u to negative values so only the second delta function of Eq. (7.8) remains. The fermion distribution functions limit the integration to regions in which $\mathbf{p}\cdot\mathbf{q}/m<0$. This means that only the first of the delta functions in Eq. (7.5) can contribute. If we average over polarizations and express momenta in units of p_F and energies in units of ϵ_F we obtain the simple expression

$$4\pi\ \mathrm{Im}\sigma_T=\frac{\sigma_0}{\omega^3}\int d^3p\int d^3q\,\delta(\omega-\Omega_p-2\mathbf{p}\cdot\mathbf{q}-q^2),$$

$$|\mathbf{p}|<1,\quad |\mathbf{p}+\mathbf{q}|>1,\quad q<q_c=\Omega_p/2,$$

where

$$\sigma_0=e^4\Omega_p p_F^4/12\pi^3 m,$$

and we have expressed q_c in terms of Ω_p using Eq. (7.1) in the limit of small q_c. Except for the trivial average over polarizations this is Eq. (55) of Tzoar and Klein,[6] but these authors neglected to cut off the plasmon momentum at q_c. For $q_c\ll 1$ integral can be evaluated to give

$$4\pi\ \mathrm{Im}\sigma_T=\frac{\pi^2}{4}\frac{\sigma_0(\Delta\omega)}{\omega^3}[\Omega_p^2-(\Delta\omega)^2] \quad \text{if} \quad 0\le\Delta\omega\le\Omega_p,$$

$$\mathrm{Im}\sigma_T=0 \quad \text{if} \quad \Delta\omega>\Omega_p,$$

where $\Delta\omega=\omega-\Omega_p$.

The effect of introducing a cutoff at q_c may be seen by looking at some numerical results. Both calculations predict a threshold for this process at the plasma frequency. The cross section then rises to a peak, which with cutoff comes at $\omega=\frac{4}{3}\Omega_p$ and without cutoff comes at a slightly higher frequency. The values of $4\pi\ \mathrm{Im}(\sigma/\sigma_0)$ at these maxima are: for $r_s=1(\Omega_p=0.6)$ 16 without cutoff and 0.31 with cutoff, and for $r_s=2(\Omega_p=0.8)$ 8 and 0.31. The case presented in Tzoar and Klein's paper is $\Omega_p=2$, corresponding to $r_s=10$, for which the perturbation theory does not converge and the results can have no quantitative significance. If we apply our formula at this value of r_s, we still find the peak reduced by the cutoff. In addition, one would expect that the plasmon resonance would be greatly broadened by collision effects which have not been included here. Strictly speaking, one must consider all contributions from the two-pair final states, which include plasmon-pair states (as mentioned above), to see if the plasmon-pair peak can be detected.

VIII. SUMMARY AND CONCLUDING REMARKS

We have seen that two-particle collision effects, which are outside the random phase, or simple pair, approximation, are the principal damping mechanism for both transverse and longitudinal electromagnetic waves in weakly interacting plasmas. This is because the one-particle damping process of the random phase approximation is zero in the transverse case and exponentially small for $k\ll k_D$ in the case of plasmons. The essential significance of the Landau damping of plasmons is to provide a short-wavelength cutoff ($k\lesssim 0.3k_D$) below which plasmons (and plasma oscillations) are strongly damped and thus poorly defined. For longer wavelengths the collision damping is, as we have seen, the principal mechanism by which plasmons transfer energy to the single particle motion.

The presence of discrete positive ions has two important effects on the collision damping rates (in contrast to the weak effect on Landau damping). First, and most important, the electron-ion collisional process produces a finite damping in the $k\to 0$ limit in the electron-ion plasma while the effect of electron-electron collisions is proportional to k^2. Second, the inclusion of ion dynamics introduces the factor $(q^2+1)/(q^2+2)$ in the integrand of Eq. (6.23). If ion screening were neglected this factor would be replaced by 1. Since the energy (or frequency) transfer in electron-ion scattering is small the ions have time to respond and contribute significantly to the total screening. This effect was first correctly calculated by Perel and Eliashberg[5] who, however, did not evaluate the integral analogous to the z integral of our Eq. (6.22).

Our calculations of the damping rate or the equivalent local conductivity are exact in the limit $k\to 0$, with $k/\omega\ll 1$, in the case of high temperatures ($kT\gg 1$ Ry) and low densities. To extend the exact theory beyond the Born approximation and therefore to lower temperatures is relatively straightforward for the electron gas where one must sum over all ladder diagrams between the colliding particles. This has the effect of replacing k_T^{-1} in Eqs. (6.28) and (6.29) by the classical distance of closest approach $e^2\beta$ in the case $e^2\beta\gg k_T^{-1}$. In intermediate regions a detailed calculation must be carried out and the result will be more complicated. For ion-electron collisions there is no distance of closest approach and there is no completely classical limit. To go beyond the Born approximation in this case one must take into account the bound states of electrons and ions in a plasma, a problem which has not yet received a satisfactory solution.

The field-theoretic approach allows us to give a complete perturbation theory of the quantized wave excitations in a plasma. Macroscopic electromagnetic waves are coherent superpositions of plasmons or

photons which are emitted or absorbed in quantized units. Thus, for example, Landau damping is just a linear process in which the collective plasmon gives up its energy to a single electron.

We should point out that our perturbation theory may be extended to treat quadratic and higher terms in the amplitude of macroscopic waves, i.e., we also can develop a perturbation theory in the wave amplitude. We can include on the right side of Eq. (3.1) terms with higher powers of E whose coefficients introduce open diagrams such as Fig. 13 representing the interaction of two plasmons ending in a single-pair state. Such a process may be thought of as a nonlinear Landau damping and appears to be related to the recent work of Montgomery and Gorman.[31] Again it appears that nonlinear collisional processes is more important than the nonlinear Landau damping. These nonlinear effects may be very important in limiting the growth of waves in instability problems. As we pointed out in Sec. V the phenomena of unstable growing waves can be understood in our approach as the net emission of quanta in the case of certain nonequilibrium distributions of states. Thus, the theory given here and the extension of it to nonlinear terms should be a powerful tool for studying both the general conditions for growing waves and the nonlinear processes which limit them.

Several rather straightforward problems remain to be treated in this theory. One is the calculation of the frequency shifts due to collisions. This can be easily carried out starting with our expressions for $4\pi\,\mathrm{Im}\sigma(\mathbf{k},\omega)$, and calculating $4\pi\,\mathrm{Re}\sigma(\mathbf{k},\omega)$ from the dispersion relation

$$\omega\,\mathrm{Re}\sigma_L(\mathbf{k},\omega)=-\mathrm{P}\int_{-\infty}^{\infty}d\omega'\,\frac{\omega'}{\omega-\omega'}\,\mathrm{Im}\sigma_L(\mathbf{k},\omega')-\frac{\Omega_p^2}{4\pi},$$

which follows from Eqs. (4.10) and (3.3). The frequency shifts are then found using Eq. (3.6). We have not carried out this calculation since the frequencies in the simple pair approximation are large (in contrast to the damping rates) and collision effects will thus give small corrections in the weak-coupling limit. It would also be interesting to include the effect of a static magnetic field. In the case of weak fields where the classical orbit radius is much greater than k_T^{-1}, the magnetic field can be incorporated using a WKB approach. The effect of collisions on the properties of the acoustic ion oscillation mode in a two-temperature plasma also remains to be studied.

The return to equilibrium of a plasma is a problem of considerable current interest. Recently, Pines and Schrieffer[2] have proposed a set of coupled equations for electrons and plasmons which describe the return to equilibrium of an electron gas. Wyld and Pines[32] have shown these equations to be equivalent under certain restrictions to the equations of Rostoker and Rosenbluth,[33] Balescu,[34] and Lenard.[35] However, in the work of Pines and Schrieffer the mechanism by which long-wavelength ($k\ll k_D$) plasmons give up energy to electrons is the Landau damping process which, as we have seen, is less important in this limit than collision damping. It appears then that their equations must be modified to take the collisional process into account.

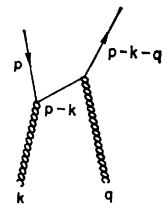

FIG. 13. Nonlinear process involving absorption of plasmons.

ACKNOWLEDGMENTS

We are grateful to Dr. W. J. Karzas for his interest and helpful remarks. We thank Richard Dolen for his critical reading of the manuscript, and also Miss Lois Foster for carrying out the numerical calculations. We are grateful to Dr. A. Ron for pointing out to us the discrepancy between the results of Dawson and Oberman and those presented in a previous version of this paper. We then discovered that the discrepancy resulted from our neglect of a diagram which has been incorporated in the present work.

Note added in proof. The paper of Dawson, Oberman, and Ron contains a number of remarks about the work of Perel and Eliashberg which convey the impression that this work is incorrect. In fact, in the limit of infinite ion mass, the only case which Perel and Eliashberg treat explicitly, Dawson, Oberman, and Ron agree exactly (despite their assertion to the contrary) with the previous result. Dawson, Oberman, and Ron do present another result for what they call the "large but finite ion mass limit." There seems to be some ambiguity about taking the limit of infinite ion mass in the completely classical case. We are not yet prepared to comment on this. However, in a recent calculation by A. Ron and N. Tzoar (to be published) in which the results of Perel and Eliashberg are extended to finite mass ratio it is shown (again despite implications to the contrary) that in the correct limit of infinite ion mass [their Eq. (44)] one obtains exactly the result of Perel and Eliashberg. The relation of this result and the second result of Dawson, *et al.*, still remains to be clarified.

[31] D. Montgomery and D. Gorman, Phys. Rev. **124**, 1309 (1961).

[32] H. W. Wyld, Jr., and D. Pines (to be published).

[33] N. Rostoker and M. N. Rosenbluth, Phys. Fluids **3**, 1 (1960).

[34] R. Balescu, Phys. Fluids **3**, 52 (1960).

[35] A. Lenard, Ann. Phys. (N. Y.) **10**, 390 (1960).